

JET PROPULSION LABORATORY

SIRTF IPF REPORT

JPL ID001095

October 17, 2003

**SIRTF INSTRUMENT POINTING FRAME
KALMAN FILTER EXECUTION SUMMARY**

IPF RUN NUMBER: 001095

REPORT TYPE: IOC EXECUTION (COARSE)

PRIME FRAME: MIPS_24um_center (95)

INFERRRED FRAMES: (96) (99) (100) (103) (104)

IPF TEAM

Autonomy and Control Section (345)

Jet Propulsion Laboratory

California Institute of Technology

4800 Oak Grove Drive

Pasadena, CA 91109

Contents

1 IPF EXECUTION SUMMARY	5
2 IPF INPUT FILE HISTORY	9
3 IPF EXECUTION RESULTS	10
3.1 IPF EXECUTION OUTPUT PLOTS	10
3.2 IPF OUTPUT DATA (IF MINI FILE)	33
3.3 IPF EXECUTION LOG	37
4 COMMENTS	40

List of Figures

1.1 A-priori and a-posteriori IPF frames	5
1.2 A-priori and a-posteriori IPF frames (ZOOMED)	8
2.1 Scenario Plot	9
3.1 TPF coords of measurements and a-priori predicts	12
3.2 Oriented PixelCoords of measurements and a-priori predicts	12
3.3 Oriented (W,V) PixelCoords of A-Priori Prediction Error Quiver Plot	13
3.4 A-priori prediction error (Science Centroids)	13
3.5 Oriented PixelCoords of measurements and a-priori predicts (PCRS only)	14
3.6 Oriented PixelCoords of measurements and a-priori predicts (Zoomed, PCRS only)	14
3.7 Oriented (W,V) PixelCoords of A-Priori PCRS Prediction Error Quiver Plot	15
3.8 A-priori PCRS prediction error	15
3.9 IPF execution convergence, chart 1	16
3.10 IPF execution convergence, chart 2	16
3.11 Parameter uncertainty convergence	17
3.12 IPF parameter symbol table	17
3.13 KF parameter error sigma plots	18
3.14 LS parameter error sigma plot	18
3.15 KF and LS parameter error sigma plot	19
3.16 Oriented PixelCoords of meas. and a-posteriori predicts	20
3.17 Oriented PixelCoords of meas. and a-posteriori predicts (attitude corrected)	20

3.18	KF innovations with (o) and w/o (+) attitude corrections	21
3.19	Histograms of science a-posteriori residuals (or innovations)	21
3.20	KF innovations with (o) and w/o (+) attitude corrections (PCRS)	22
3.21	Histograms of PCRS a-posteriori residuals (or innovations)	22
3.22	A-Posteriori Science Centroid Prediction Error Quiver (Att. Cor.)	23
3.23	Normalized A-Posteriori Science Centroid Prediction Errors	23
3.24	A-Posteriori PCRS Prediction Errors Quiver (Att. Cor.)	24
3.25	Normalized A-Posteriori PCRS Prediction Errors	24
3.26	W-axis KF innovations and 1-sigma bound	25
3.27	V-axis KF innovations and 1-sigma bound	25
3.28	Array plot with (solid) and w/o (dashed) optical distortion corrections	26
3.29	Optical Distortion Plot: total (x5 magnification)	26
3.30	Optical Distortion Plot: constant plate scales (x5 magnification)	27
3.31	Optical Distortion Plot: linear plate scale (x5 magnification)	27
3.32	Optical Distortion Plot: gamma terms (x5 magnification)	28
3.33	Estimated attitude corrections (Body frame)	29
3.34	Estimated attitude error sigma plot (Body frame)	29
3.35	Thermo-mechanical boresight drift (equiv. angle in (W,V) coords)	30
3.36	Thermo-mechanical boresight drift (equiv. angle in Body frame)	30
3.37	Gyro drift bias contribution (equiv. rate in (W,V) coords)	31
3.38	Gyro drift bias contribution (equiv. angle in (W,V) coords)	31
3.39	Gyro drift bias contribution (equiv. angle in Body frame)	32

List of Tables

1.1	IPF filter input files	6
1.2	IPF filter execution configuration	6
1.3	IPF filter execution mask vector assignment	6
1.4	IPF calibration error summary ([arcsec], 1-sigma, radial)	7
1.5	Measurement prediction error summary (1-sigma)	7
1.6	IPF Brown angle summary	8
2.1	IPF input file editing status	9
3.1	Table of figures I (IPF run)	10

3.2 Table of figures II (IPF run)	11
---	----

1 IPF EXECUTION SUMMARY

This report summarizes the SIRTF Instrument Pointing Frame (IPF) Kalman Filter execution associated with run file: RN001095. In particular, this Focal Point Survey calibrates the instrument: MIPS_24um_center (95), as part of the IOC Coarse Survey. The main calibration results from the IPF filter execution have been documented in IF001095 typically stored in the mission archive DOM collection IPF.IF. This report only summarizes the main aspects of the run, and does not substitute for the full information contained in the IF file.

Section 1 summarizes the filter execution results. The filter configurations are tabulated in Table 1.2 and the mask vector assignments are tabulated in Table 1.3. A total of 27 state parameters are estimated in this run. The overall End-to-End pointing performances are tabulated in Table 1.4. The prediction residuals throughout the estimation processes are tabulated in Table 1.5. Section 3 summarizes resulting plots, a mini summary of the IF IPF output file, and the execution log. Section 4 captures the user comments that are specific to this particular run.

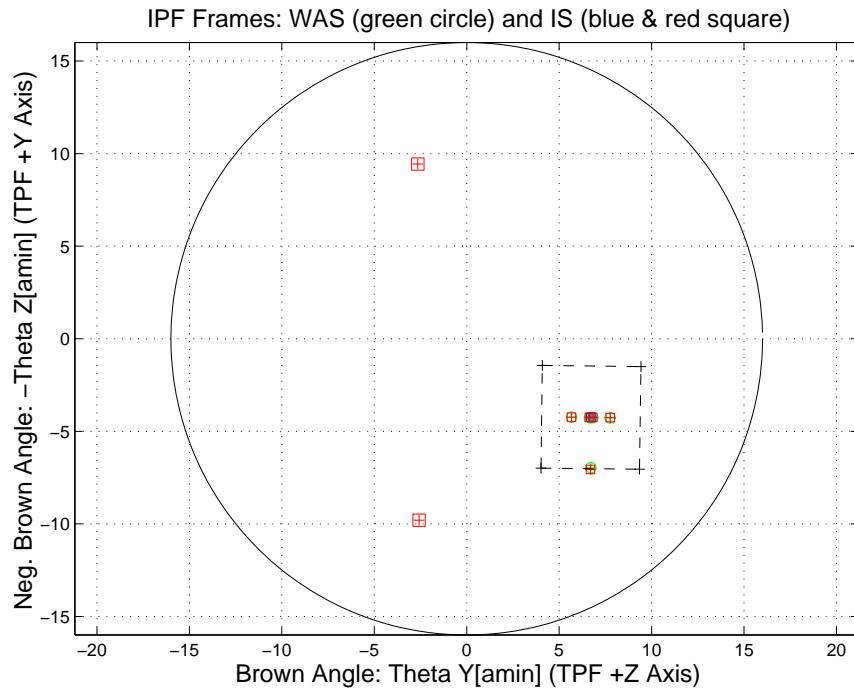


Figure 1.1: A-priori and a-posteriori IPF frames

RAW	FINAL (After Editing)
AA001095	AA001095
AS001095	AS001095
CA003095	CA003095
CB002095	CB002095
CS003095	CS003095

Table 1.1: IPF filter input files

EXECUTION CONFIGURATION ITEM	CURRENT STATUS
IPF Filter Version Used	IPF.V2.0.0D
Frame Table Version Used	BodyFrames_SPC_08a
Scan-Mirror Employed?	YES
IPF Filter Mode	NORMAL-MODE(0)
SLIT-MODE Operation	DISABLED
Kalman Filter Operation	ENABLED
Least-Squares Data Analysis	ENABLED
IBAD Screening	ENABLED
User-Specified Data Editing	DISABLED
Total Number of Iterations	30
LS Residual Sigma Scale	1.05547971E+000
Total Number of Maneuvers	7

Table 1.2: IPF filter execution configuration

Con. Plate Scale			Γ Dependent				Γ^2 Dependent				Linear Plate Scale						Mirror			
a_{00}	b_{00}	c_{00}	a_{10}	b_{10}	c_{10}	d_{10}	a_{20}	b_{20}	c_{20}	d_{20}	a_{01}	b_{01}	c_{01}	d_{01}	e_{01}	f_{01}	α	β		
1	2	3	4	5	6	7	8	9	10	11	12	13	14	15	16	17	18	19		
1	1	1	1	1	1	1	0	0	0	0	1	1	1	1	1	1	1	1		
IPF (T)			Alignment R						Gyro Drift Bias											
θ_1	θ_2	θ_3	a_{rx}	a_{ry}	a_{rz}	b_{rx}	b_{ry}	b_{rz}	c_{rx}	c_{ry}	c_{rz}	b_{gx}	b_{gy}	b_{gz}	c_{gx}	c_{gy}	c_{gz}			
20	21	22	23	24	25	26	27	28	29	30	31	32	33	34	35	36	37			
1	1	1	1	1	1	0	0	0	0	0	0	1	1	1	1	1	1			

Table 1.3: IPF filter execution mask vector assignment

FOCAL PLANE SURVEY ANALYSIS: IOC Coarse Survey.

INSTRUMENT NAME: MIPS_24um_center NF: 95

PIX2RADW: 1.20874169E-005 [rad/pixel] = 2.4932E+000 [arcsec/pixel]

PIX2RADV: 1.20874169E-005 [rad/pixel] = 2.4932E+000 [arcsec/pixel]

FRAME	DESCRIPTION	IPF ¹	SF ²	TOTAL	REQ
095(P)	MIPS_24um_center	0.0988	0.0855	0.1307	1.00
096(I)	MIPS_24um_plusY_edge	0.1258	0.0855	0.1521	N/A
099(I)	MIPS_24um_small_FOV1	0.1008	0.0855	0.1322	N/A
100(I)	MIPS_24um_small_FOV2	0.0986	0.0855	0.1305	N/A
103(I)	MIPS_24um_large_FOV1	0.0989	0.0855	0.1307	N/A
104(I)	MIPS_24um_large_FOV2	0.0987	0.0855	0.1306	N/A

Table 1.4: IPF calibration error summary ([arcsec], 1-sigma, radial)

RMS METRIC	A PRIORI ³	A POSTERIORI ³	ATT. CORRECTED ⁴	UNITS
Radial	2.3439	0.3786	0.1557	arcsec
W-Axis	1.3088	0.2156	0.0846	arcsec
V-Axis	1.9445	0.3112	0.1307	arcsec
Radial	0.9401	0.1519	0.0625	pixels
W-Axis	0.5249	0.0865	0.0339	pixels
V-Axis	0.7799	0.1248	0.0524	pixels

Table 1.5: Measurement prediction error summary (1-sigma)

¹IPF filter removes systematic pointing errors due to: thermomechanical alignment drift (Body to TPF), gyro bias and bias drift, centroiding error, attitude error, and optical distortion. IPF SIGMA presented here is “Scaled” by the Least Squares Scale factor. The Least Squares Scale Factor was: 1.055480. It is assumed that the gyro Angle Random Walk contribution is captured with the Least Squares scaling. The gyro ARW contribution can be approximately calculated as 0.0756 arcseconds, given that ARW = 100 $\mu\text{deg}/\sqrt{\text{hr}}$, with 5.553000e+002 second Maneuver time (max), and 7 independent Maneuvres.

²Gyro Scale Factor(GSF) assumes 95 ppm error over 0.250 degree maneuver.

³This can be interpreted as estimate of ”pixel to sky” pointing reconstruction error if no science data is used.

⁴This can be interpreted as estimate of achieved S/I centroiding error

IPF BROWN ANGLE SUMMARY					
FRAME TABLE USED: BodyFrames_SPC_08a					
NF	NAME	WAS	IS	CHANGE	UNIT
095	theta_Y	+6.724001	+6.718185	-0.005816	arcmin
095	theta_Z	+4.258239	+4.247276	-0.010963	arcmin
095	angle	+0.577299	+0.638444	+0.061144	deg
096	theta_Y	+6.721218	+6.695268	-0.025950	arcmin
096	theta_Z	+6.970374	+7.063358	+0.092984	arcmin
096	angle	+0.577299	+0.638444	+0.061144	deg
099	theta_Y	+7.758095	+7.758870	+0.000775	arcmin
099	theta_Z	+4.277861	+4.260684	-0.017177	arcmin
099	angle	+0.577299	+0.638444	+0.061144	deg
100	theta_Y	+5.669225	+5.661628	-0.007597	arcmin
100	theta_Z	+4.238226	+4.235185	-0.003040	arcmin
100	angle	+0.577299	+0.638444	+0.061144	deg
103	theta_Y	+6.827410	+6.822038	-0.005373	arcmin
103	theta_Z	+4.260201	+4.248547	-0.011654	arcmin
103	angle	+0.577299	+0.638444	+0.061144	deg
104	theta_Y	+6.641274	+6.635138	-0.006136	arcmin
104	theta_Z	+4.256670	+4.246270	-0.010400	arcmin
104	angle	+0.577299	+0.638444	+0.061144	deg

Table 1.6: IPF Brown angle summary

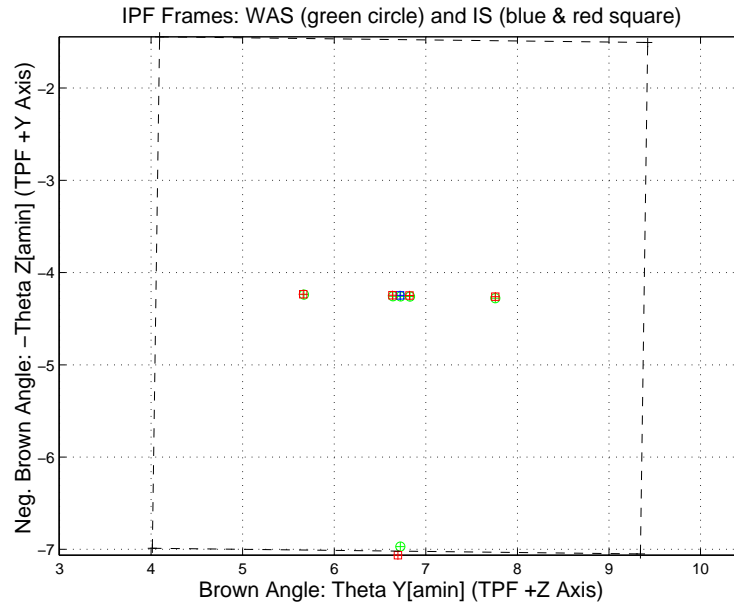


Figure 1.2: A-priori and a-posteriori IPF frames (ZOOMED)

2 IPF INPUT FILE HISTORY

WAS	SIZE	IS	SIZE	REMOVED	PATCHED
AA001095	UNCHANGED	AA001095	UNCHANGED	0	0
CA003095	UNCHANGED	CA003095	UNCHANGED	0	N/A
CB002095	UNCHANGED	CB002095	UNCHANGED	0	N/A

Table 2.1: IPF input file editing status

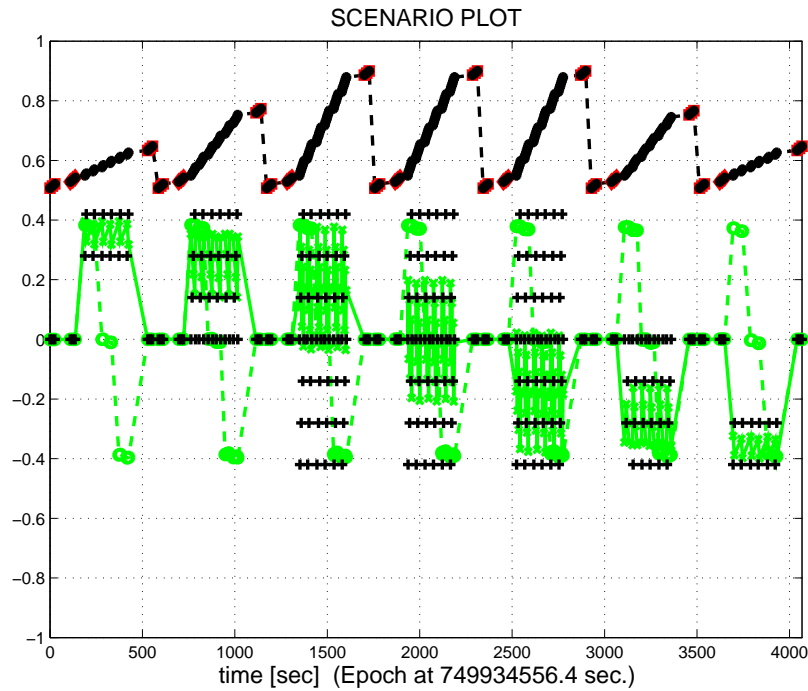


Figure 2.1: Scenario Plot

3 IPF EXECUTION RESULTS

3.1 IPF EXECUTION OUTPUT PLOTS

This subsection summarizes the IPF filter results. As shown in Table 3.1, the output plots are segmented to three groups: predicted performance, post-run results and IPF trending plots.

FIGURE NO.	DESCRIPTION
Predicted performance prior to IPF run	
Figure 3.1	Meas. and a-priori predicts in TPF coords
Figure 3.2	Meas. and a-priori predicts in Oriented Pixel Coords including rectangular array boundary approximation
Figure 3.3	A-Priori Prediction Error Quiver Plot in Oriented Pixel Coords including rectangular array boundary approximation
Figure 3.4	A-priori prediction error
Figure 3.5	Oriented Pixel Coords of measurements and a-priori predicts (PCRS only)
Figure 3.6	Oriented Pixel Coords of measurements and a-priori predicts (Zoomed, PCRS only)
Figure 3.7	Oriented (W,V) Pixel Coords of A-Priori PCRS Prediction Error Quiver Plot
Figure 3.8	A-priori PCRS prediction error
IPF filter performance (post run results)	
Figure 3.9	IPF execution convergence, chart 1: (top) normalized residual error vs. iteration number and (bottom) norm of effective parameter corrections
Figure 3.10	IPF execution convergence, chart 2: parameter correction size vs. iteration number
Figure 3.11	Parameter uncertainty convergence: square-root of diagonal elements of covariance matrix vs. maneuver number
Figure 3.12	IPF parameter symbol table
Figure 3.13	KF parameter error sigma plot (a-priori-dashed, a-posteriori-solid). Includes true parameter errors (FLUTE runs only)
Figure 3.14	LS parameter error sigma plot. Includes true parameter errors (FLUTE runs only)
Figure 3.15	KF and LS parameter errors sigma plot (Figure 3.13 & Figure 3.14 combined)
Figure 3.16	Measurements and a-posteriori predicts in Oriented Pixel Coords including rectangular array boundaries (a-priori-dashed, a-posteriori-solid)
Figure 3.17	Attitude corrected meas. and a-posteriori predicts in Oriented Pixel Coords including rectangular array boundaries (a-priori-dashed, a-posteriori-solid)

Table 3.1: Table of figures I (IPF run)

FIGURE NO.	DESCRIPTION
IPF filter performance (post run results) - CONTINUE	
Figure 3.18	KF innovations with (o) and w/o (+) attitude corrections
Figure 3.19	Histograms of science a-posteriori residuals (or innovations)
Figure 3.20	KF innovations with (o) and w/o (+) attitude corrections (PCRS)
Figure 3.21	Histograms of PCRS a-posteriori residuals (or innovations)
Figure 3.22	A-Posteriori Science Centroid Prediction Error Quiver (Att. Cor.)
Figure 3.23	Normalized A-Posteriori Science Centroid Prediction Errors
Figure 3.24	A-Posteriori PCRS Prediction Errors Quiver (Att. Cor.)
Figure 3.25	Normalized A-Posteriori PCRS Prediction Errors
Figure 3.26	W-axis KF innovations and 1-sigma bound
Figure 3.27	V-axis KF innovations and 1-sigma bound
Figure 3.28	Array plot with (solid) and w/o (dashed) optical distortion corrections
Figure 3.29	Optical Distortion Plot: total (x5 magnification)
Figure 3.30	Optical Distortion Plot: constant plate scales (x5 magnification)
Figure 3.31	Optical Distortion Plot: linear plate scale (x5 magnification)
Figure 3.32	Optical Distortion Plot: gamma terms (x5 magnification)
IPF parameter trending plots	
Figure 3.33	Estimated attitude corrections (Body frame)
Figure 3.34	Estimated attitude error sigma plot (Body frame)
Figure 3.35	Systematic error attributed to thermo-mechanical boresight drift (equiv. angle in (W,V) coords)
Figure 3.36	Systematic error attributed to thermo-mechanical boresight drift (equiv. angle in Body frame)
Figure 3.37	Systematic error attributed to gyro drift bias (equiv. rate in (W,V) coords)
Figure 3.38	Systematic error attributed to gyro drift bias (equiv. angle in (W,V) coords)
Figure 3.39	Systematic error attributed to gyro drift bias (equiv. angle in Body frame)

Table 3.2: Table of figures II (IPF run)

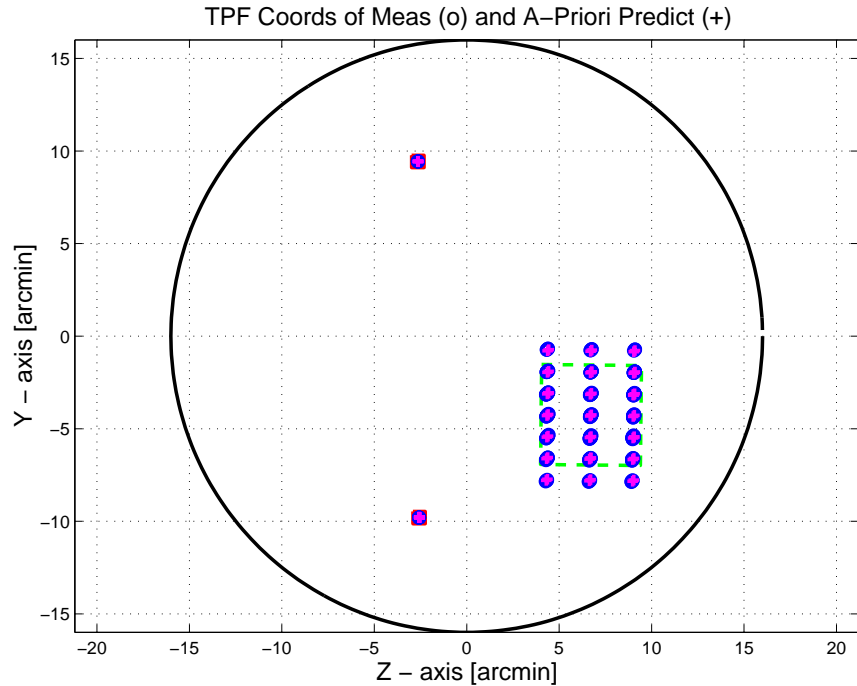


Figure 3.1: TPF coords of measurements and a-priori predicts

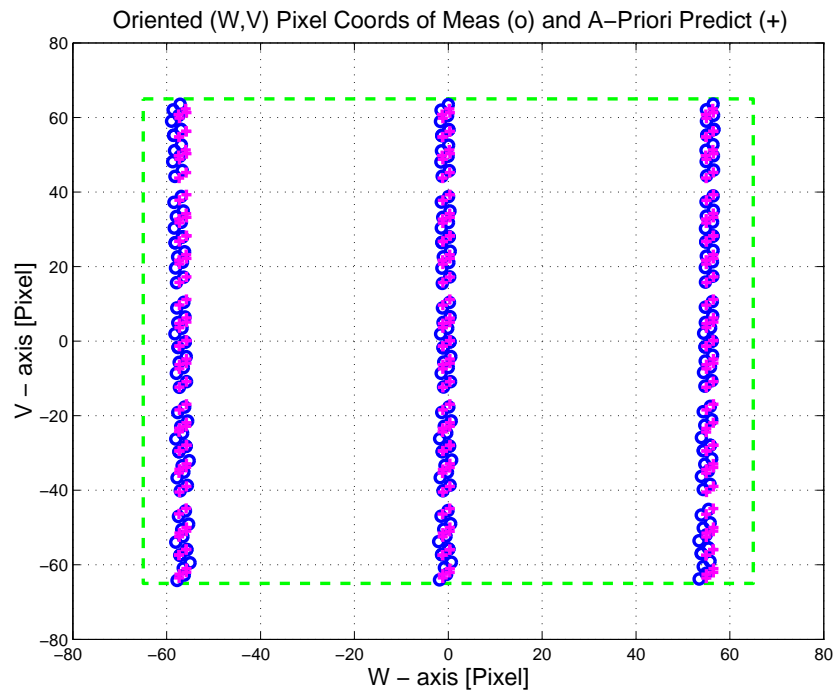


Figure 3.2: Oriented Pixel Coords of measurements and a-priori predicts

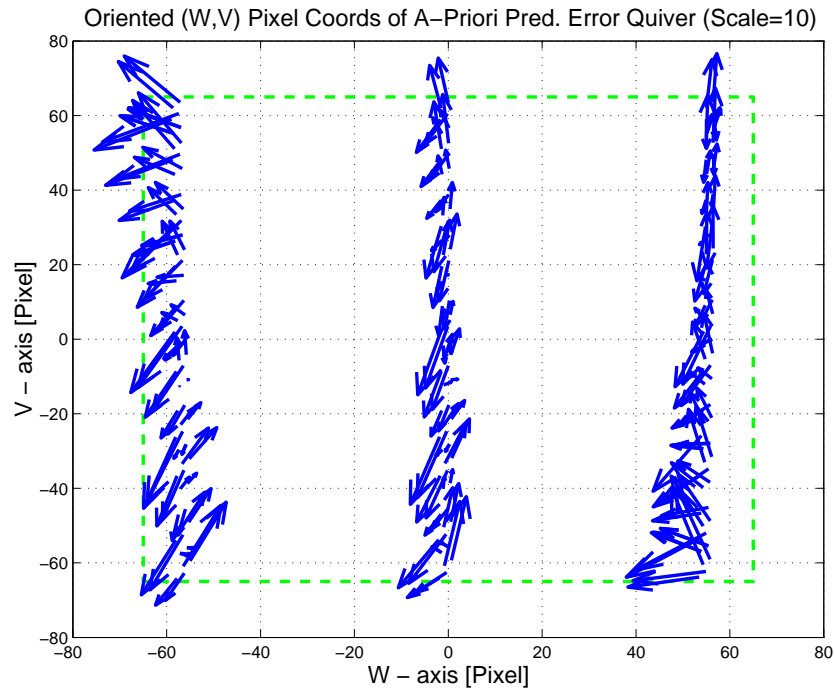


Figure 3.3: Oriented (W,V) Pixel Coords of A-Priori Prediction Error Quiver Plot

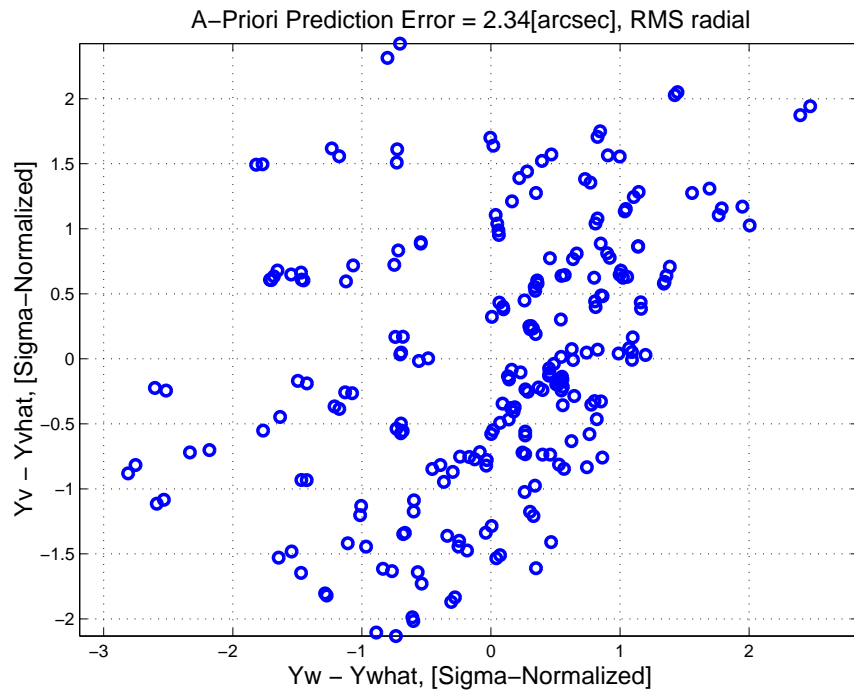


Figure 3.4: A-priori prediction error (Science Centroids)

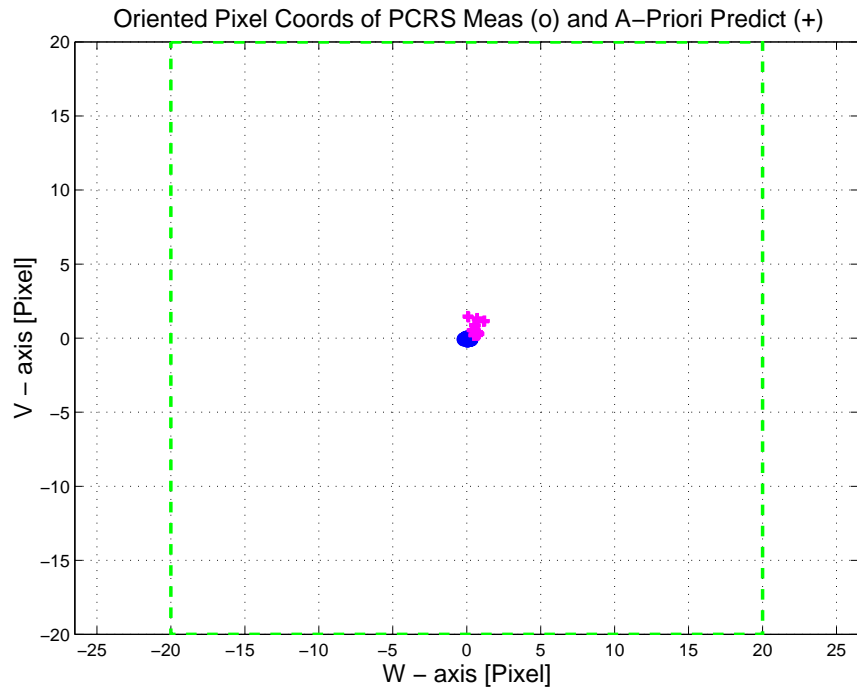


Figure 3.5: Oriented Pixel Coords of measurements and a-priori predicts (PCRS only)

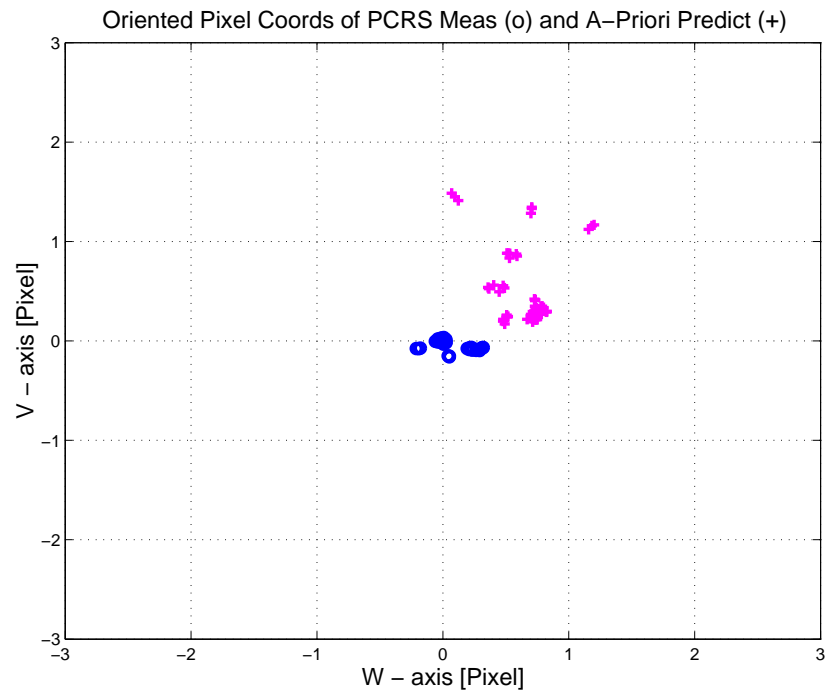


Figure 3.6: Oriented Pixel Coords of measurements and a-priori predicts (Zoomed, PCRS only)

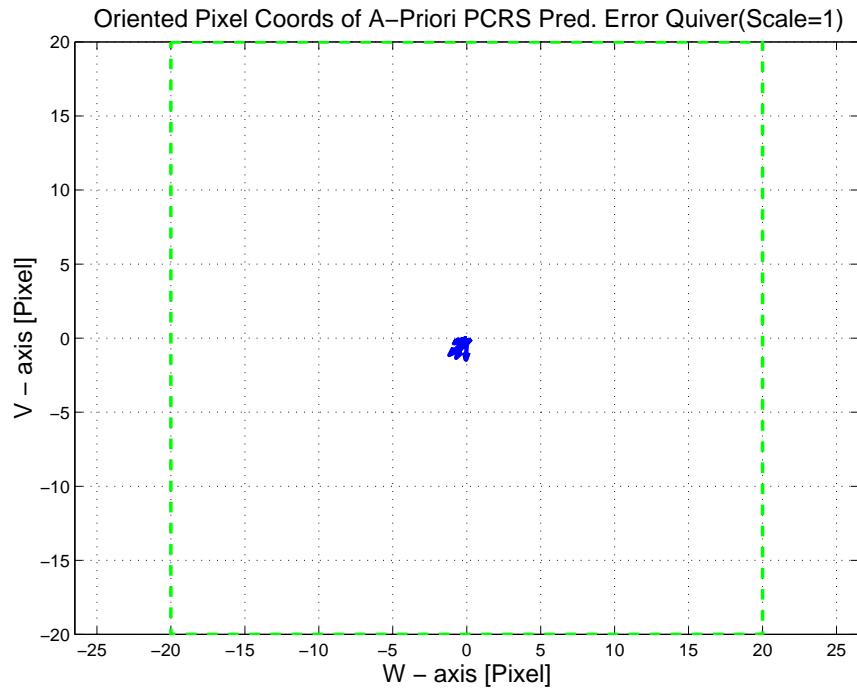


Figure 3.7: Oriented (W,V) Pixel Coords of A-Priori PCRS Prediction Error Quiver Plot

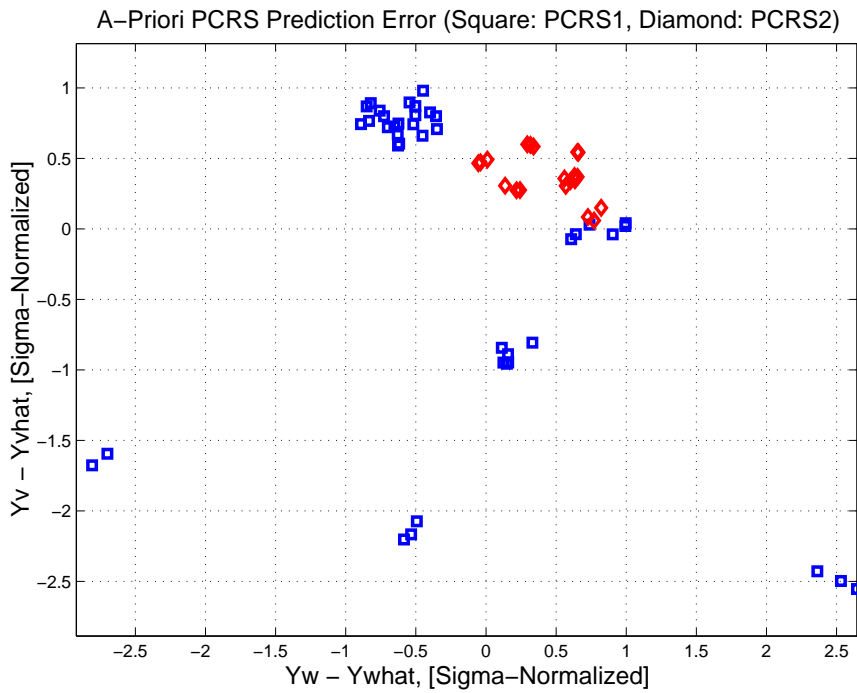


Figure 3.8: A-priori PCRS prediction error

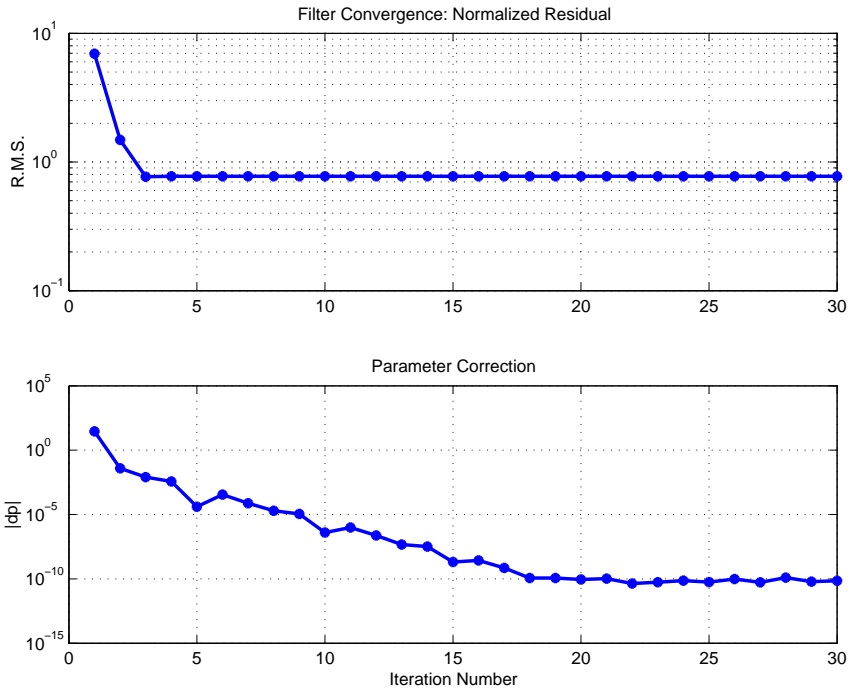


Figure 3.9: IPF execution convergence, chart 1

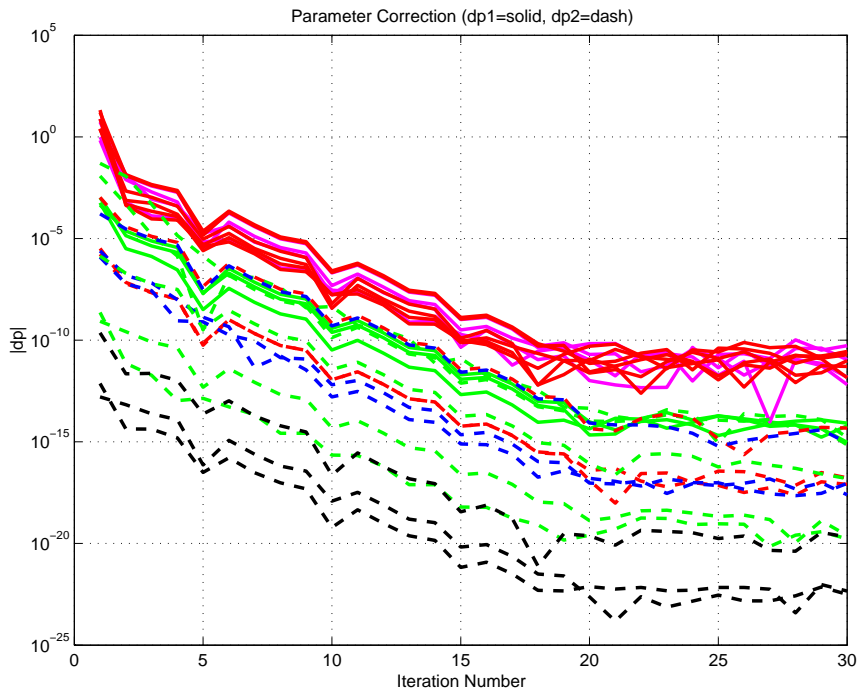


Figure 3.10: IPF execution convergence, chart 2

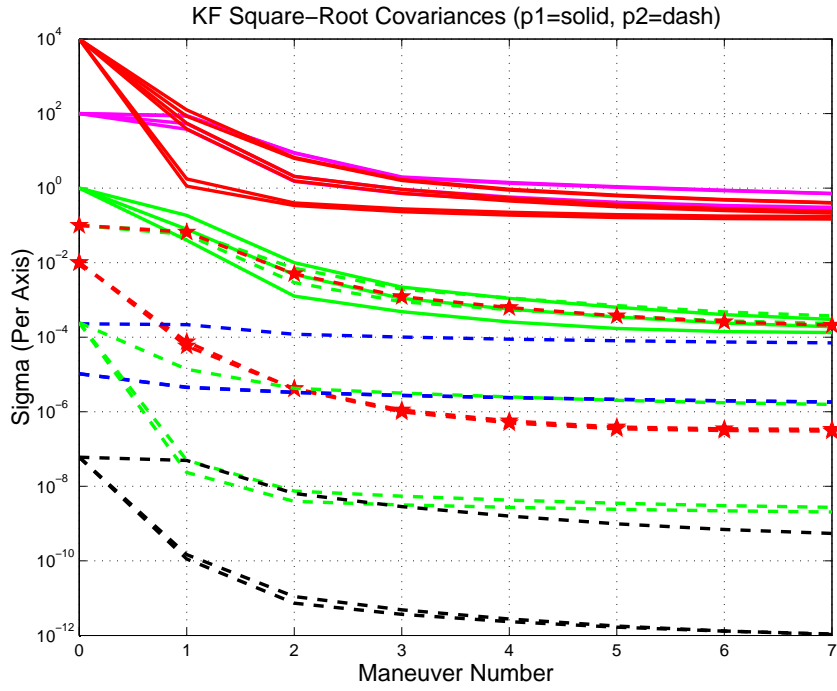


Figure 3.11: Parameter uncertainty convergence

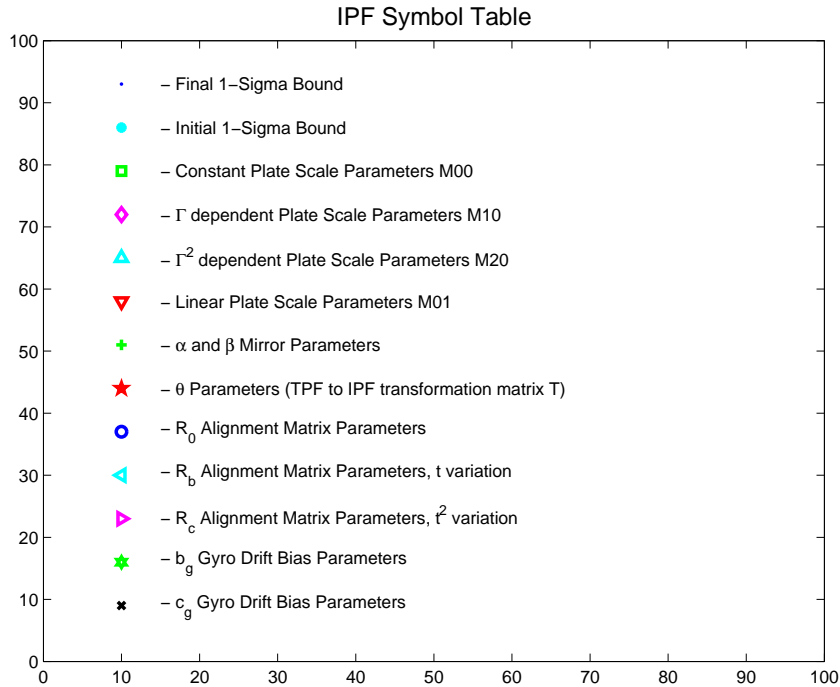


Figure 3.12: IPF parameter symbol table

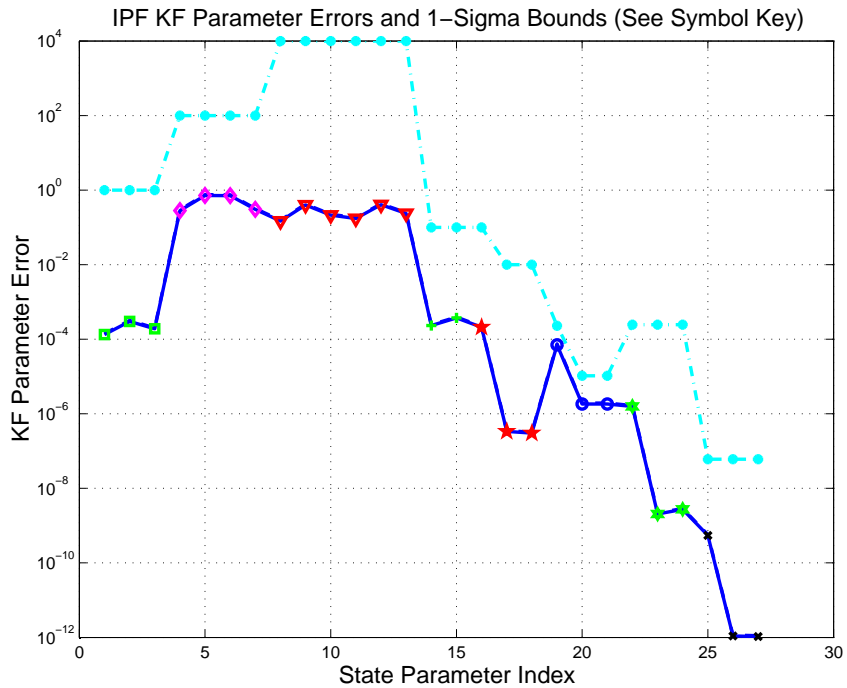


Figure 3.13: KF parameter error sigma plots

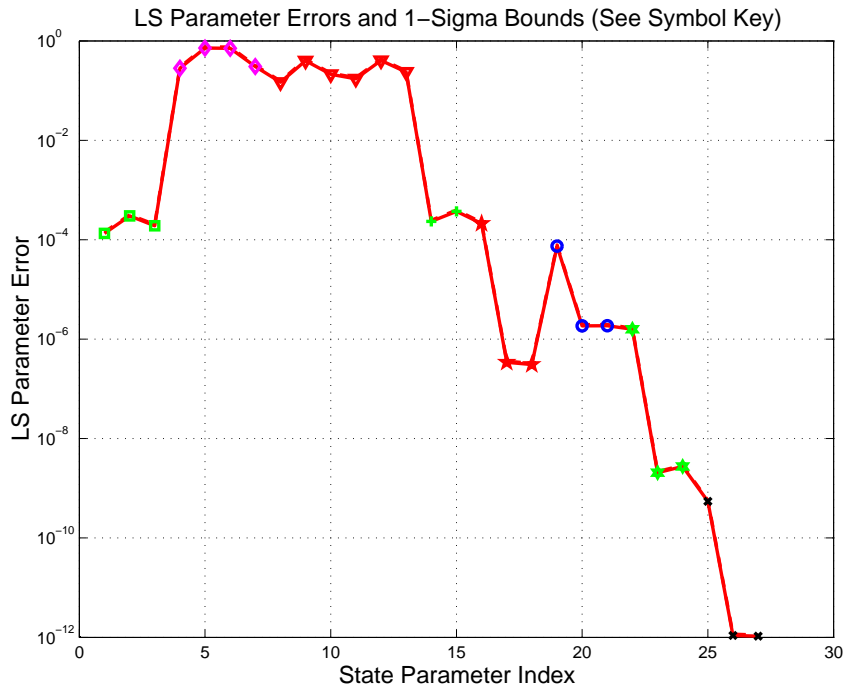


Figure 3.14: LS parameter error sigma plot

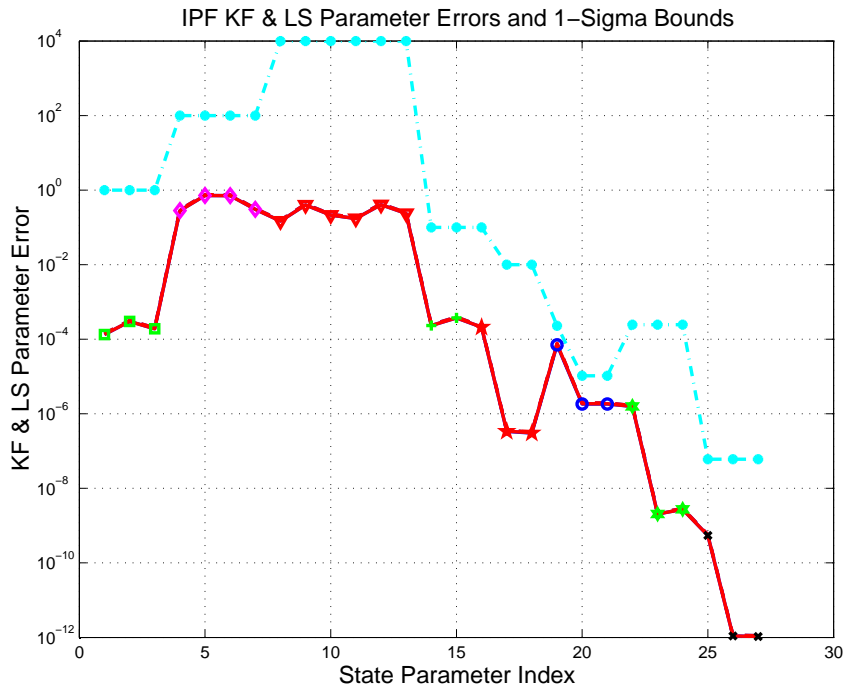


Figure 3.15: KF and LS parameter error sigma plot

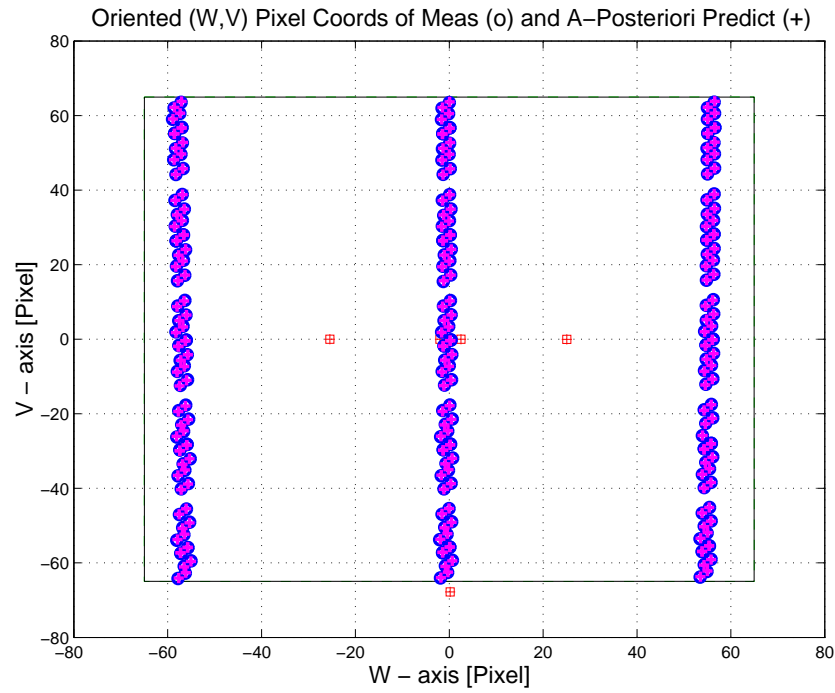


Figure 3.16: Oriented Pixel Coords of meas. and a-posteriori predicts

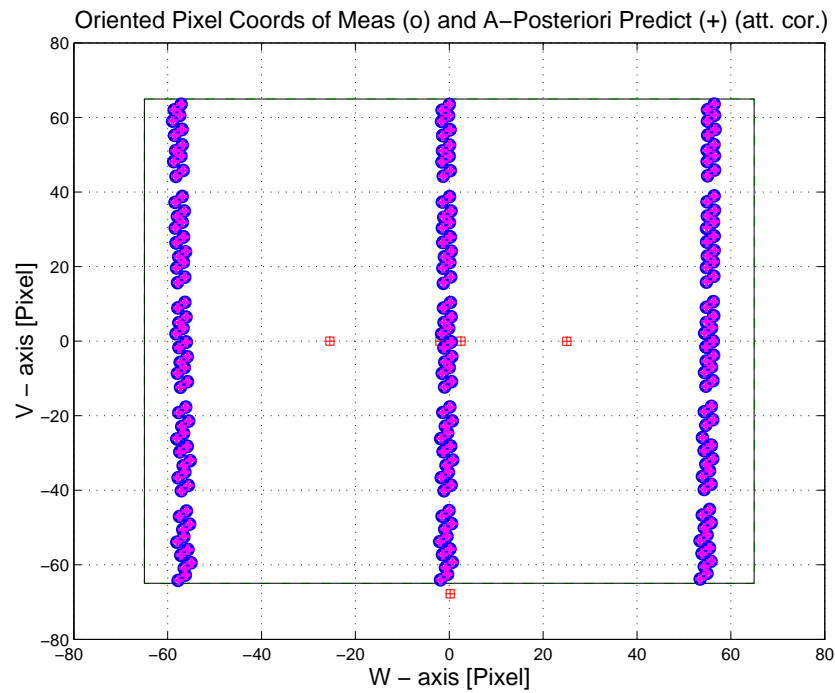


Figure 3.17: Oriented Pixel Coords of meas. and a-posteriori predicts (attitude corrected)

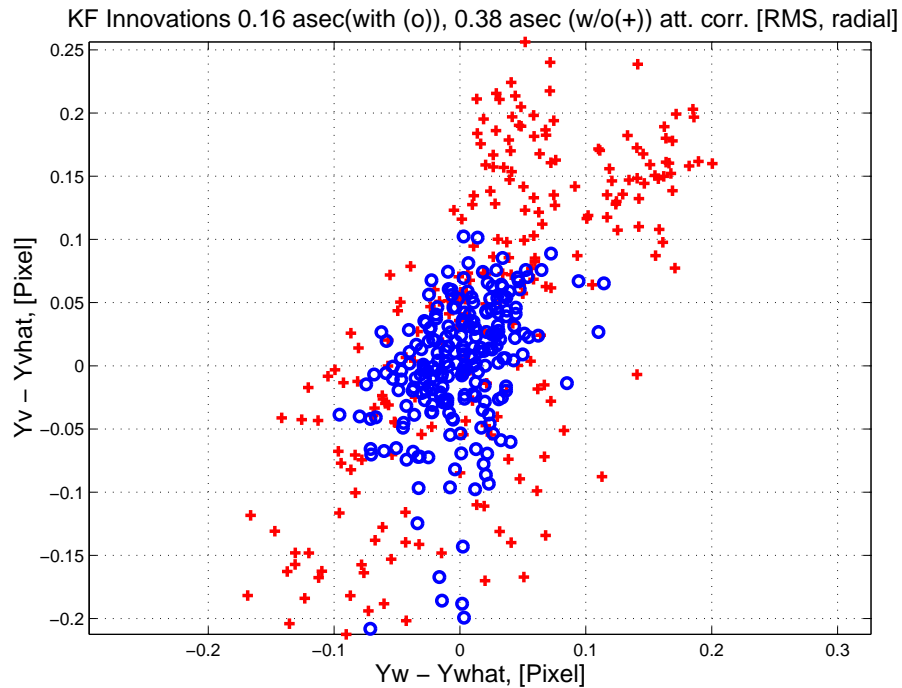


Figure 3.18: KF innovations with (o) and w/o (+) attitude corrections

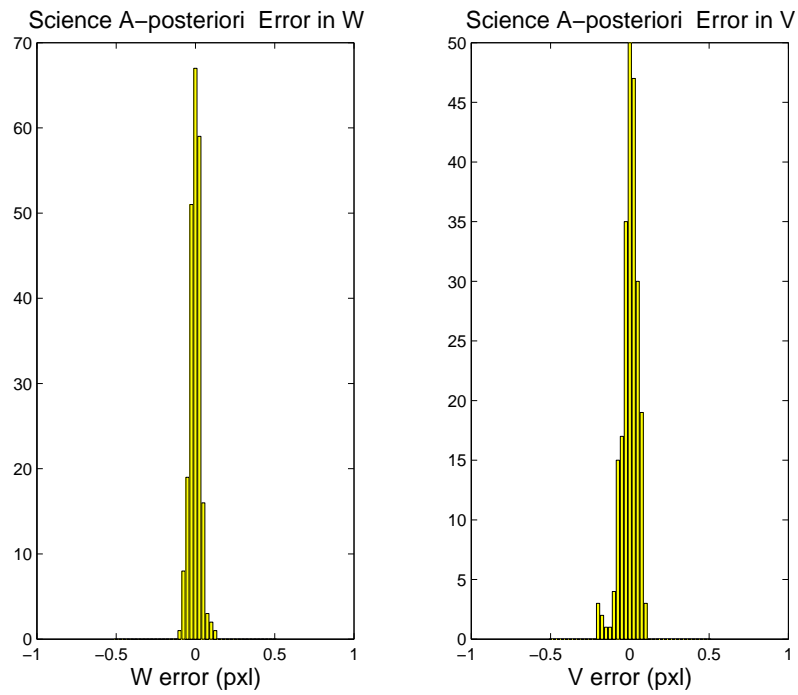


Figure 3.19: Histograms of science a-posteriori residuals (or innovations)

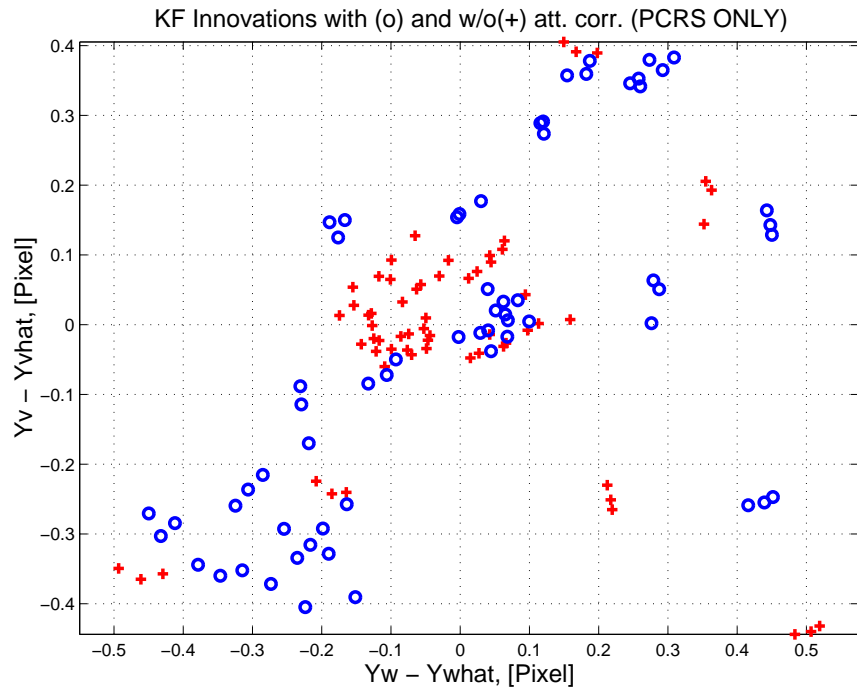


Figure 3.20: KF innovations with (o) and w/o (+) attitude corrections (PCRS)

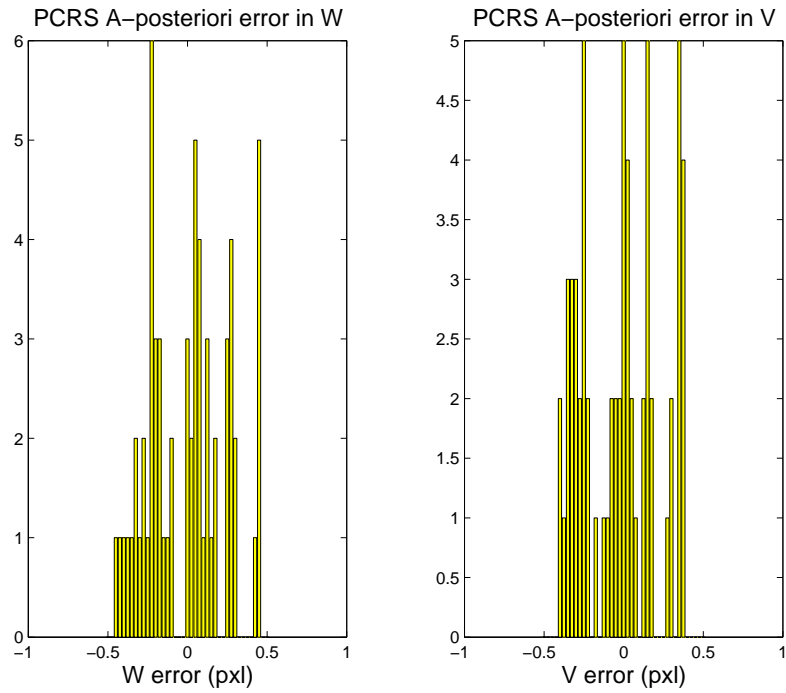


Figure 3.21: Histograms of PCRS a-posteriori residuals (or innovations)

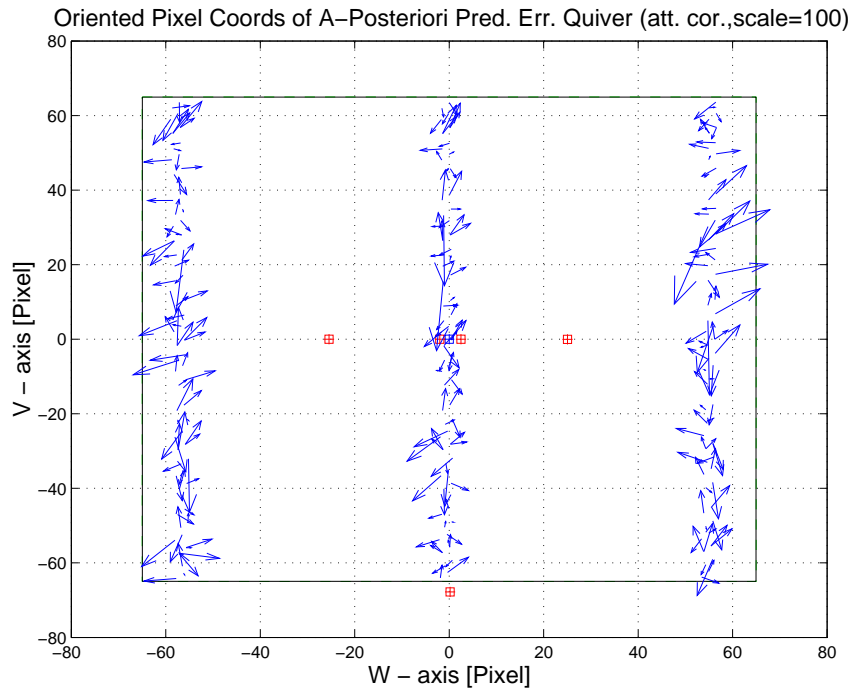


Figure 3.22: A-Posteriori Science Centroid Prediction Error Quiver (Att. Cor.)

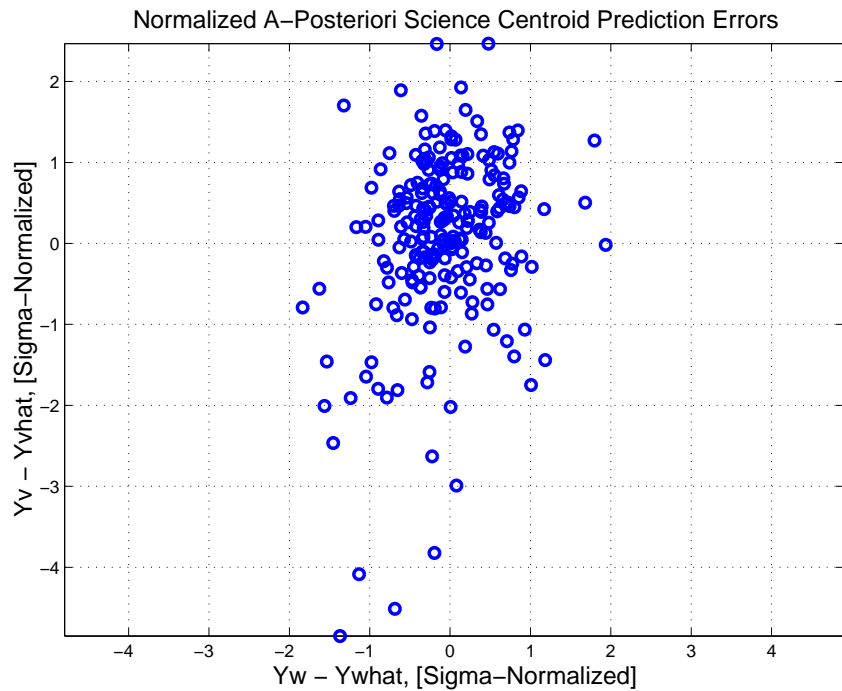


Figure 3.23: Normalized A-Posteriori Science Centroid Prediction Errors

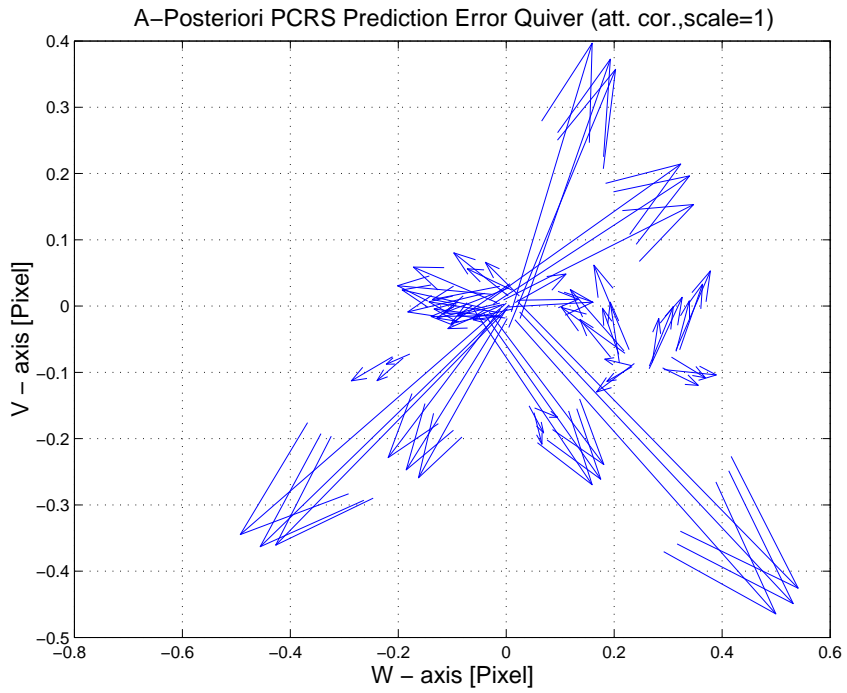


Figure 3.24: A-Posteriori PCRS Prediction Errors Quiver (Att. Cor.)

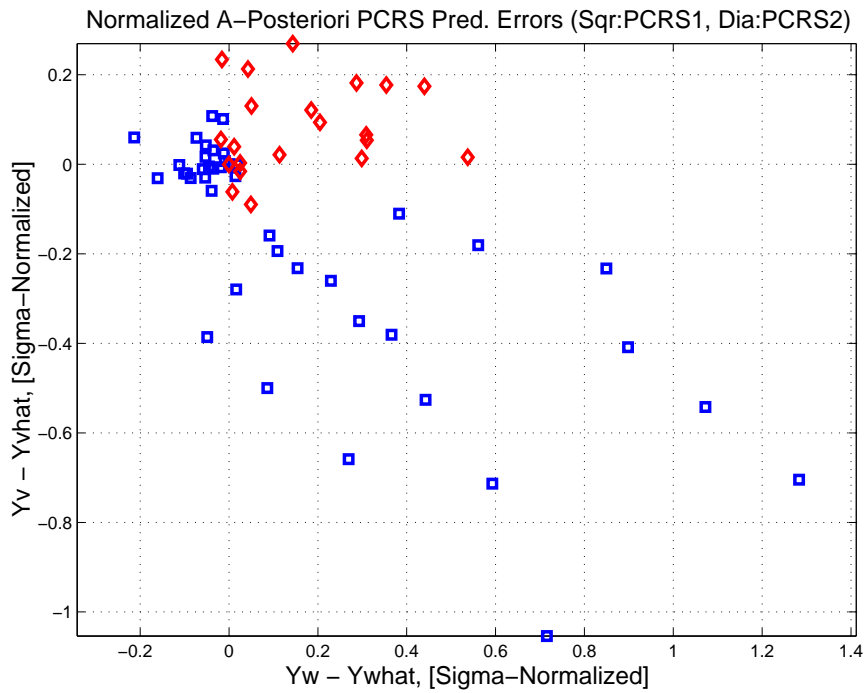


Figure 3.25: Normalized A-Posteriori PCRS Prediction Errors

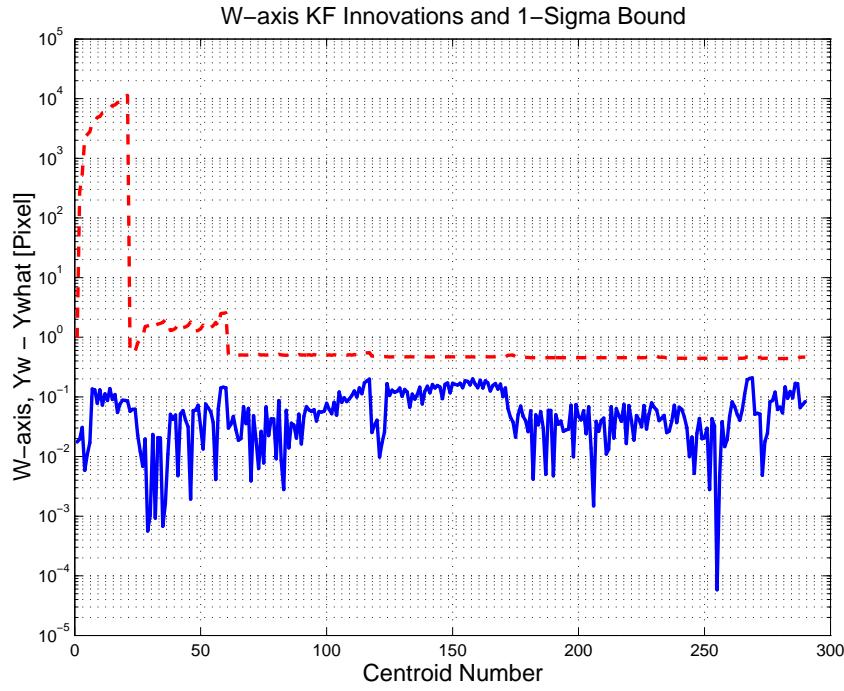


Figure 3.26: W-axis KF innovations and 1-sigma bound

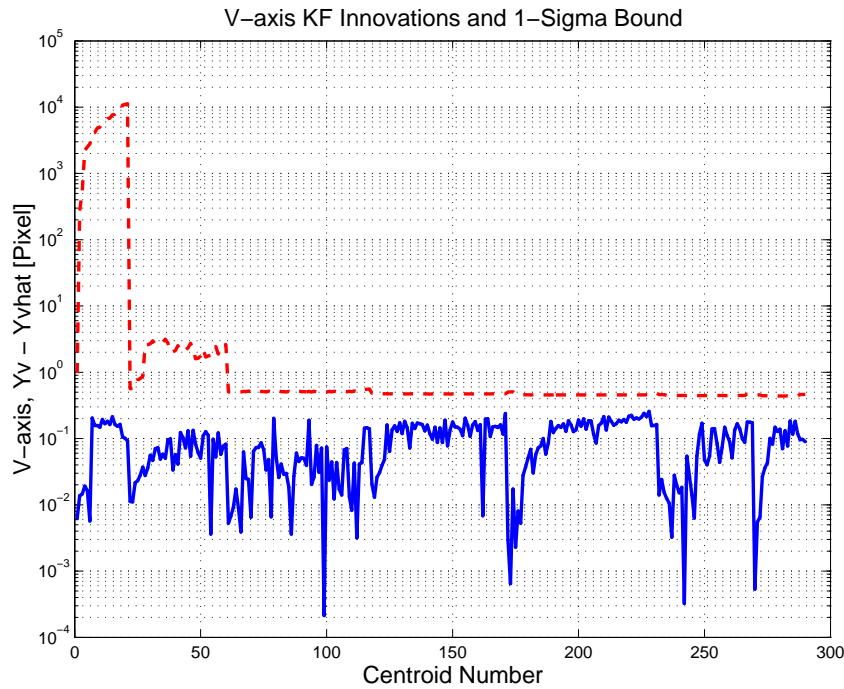


Figure 3.27: V-axis KF innovations and 1-sigma bound

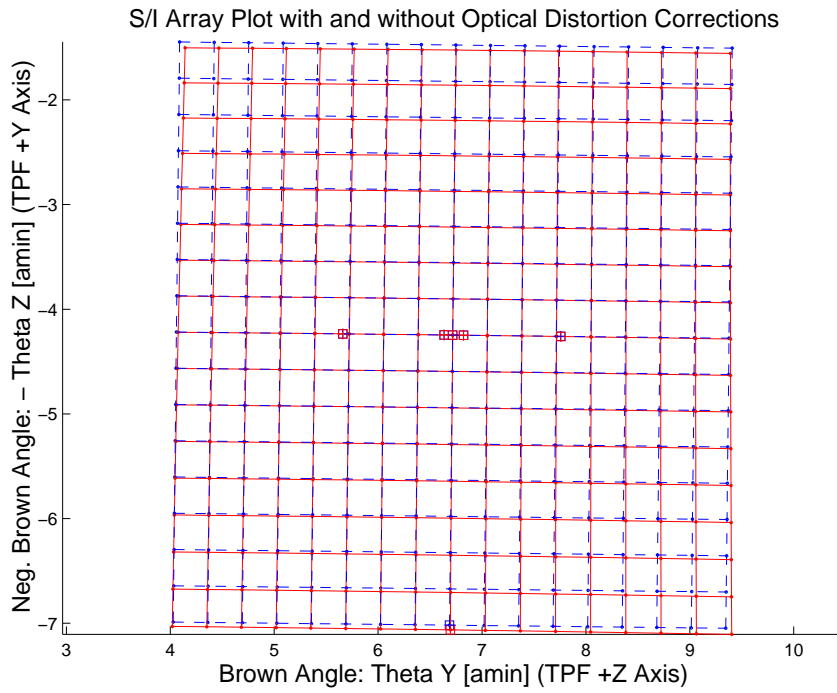


Figure 3.28: Array plot with (solid) and w/o (dashed) optical distortion corrections

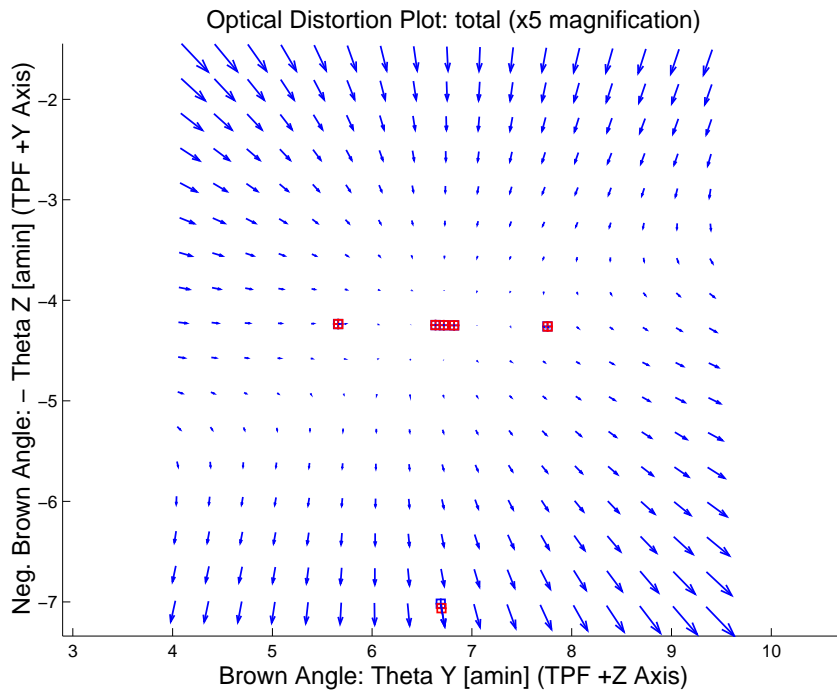


Figure 3.29: Optical Distortion Plot: total (x5 magnification)

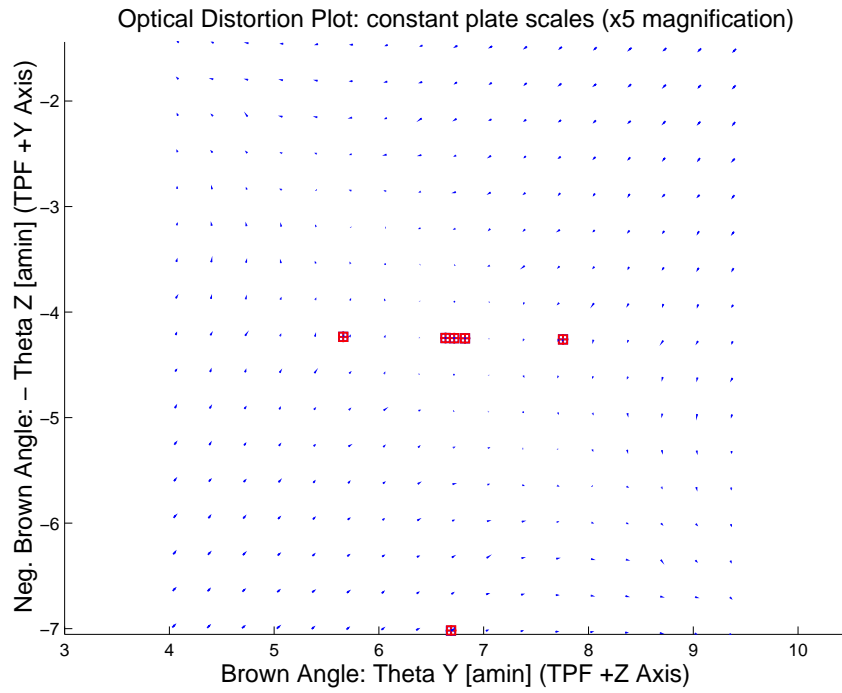


Figure 3.30: Optical Distortion Plot: constant plate scales (x5 magnification)

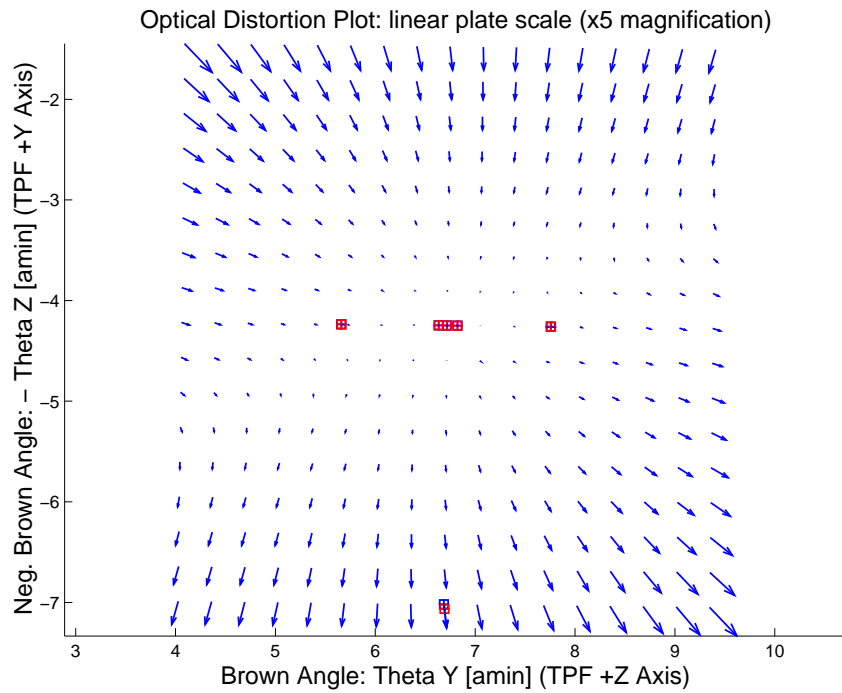


Figure 3.31: Optical Distortion Plot: linear plate scale (x5 magnification)

Opt. Dist. Plot: Γ depdt; $\Gamma = -3.99676e-004$ in blue and $\Gamma = 3.99676e-004$ in red (x5 magn)

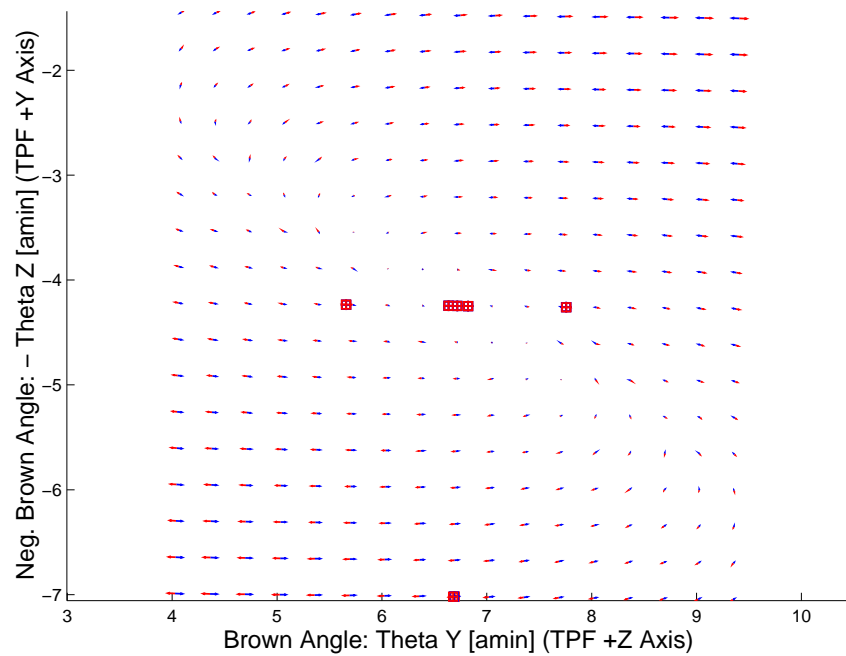


Figure 3.32: Optical Distortion Plot: gamma terms (x5 magnification)

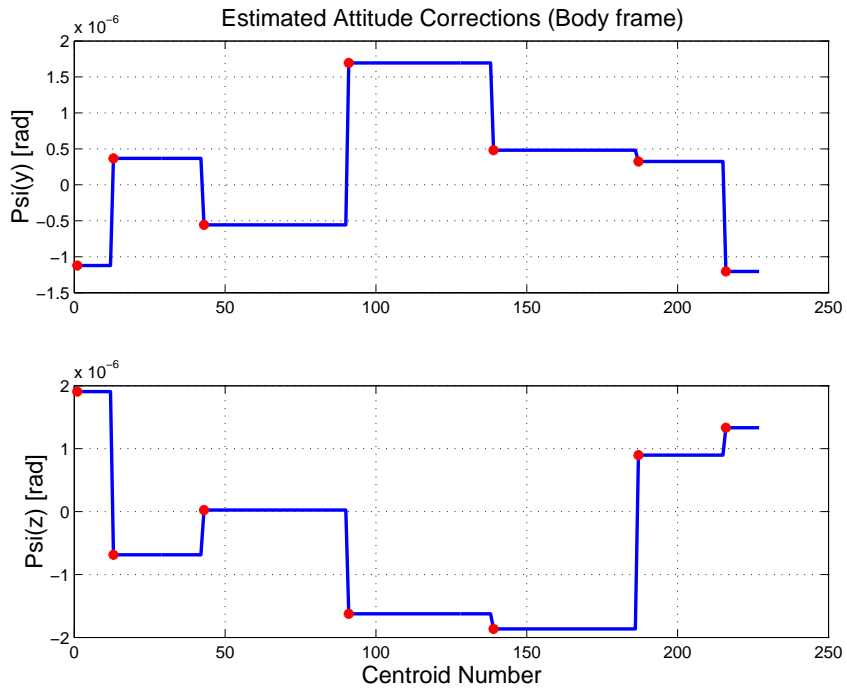


Figure 3.33: Estimated attitude corrections (Body frame)

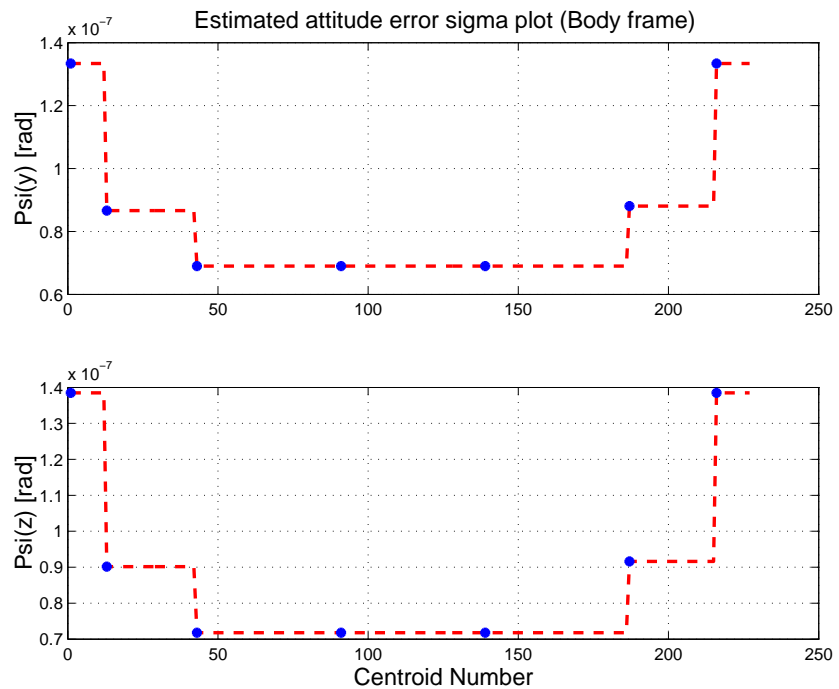


Figure 3.34: Estimated attitude error sigma plot (Body frame)

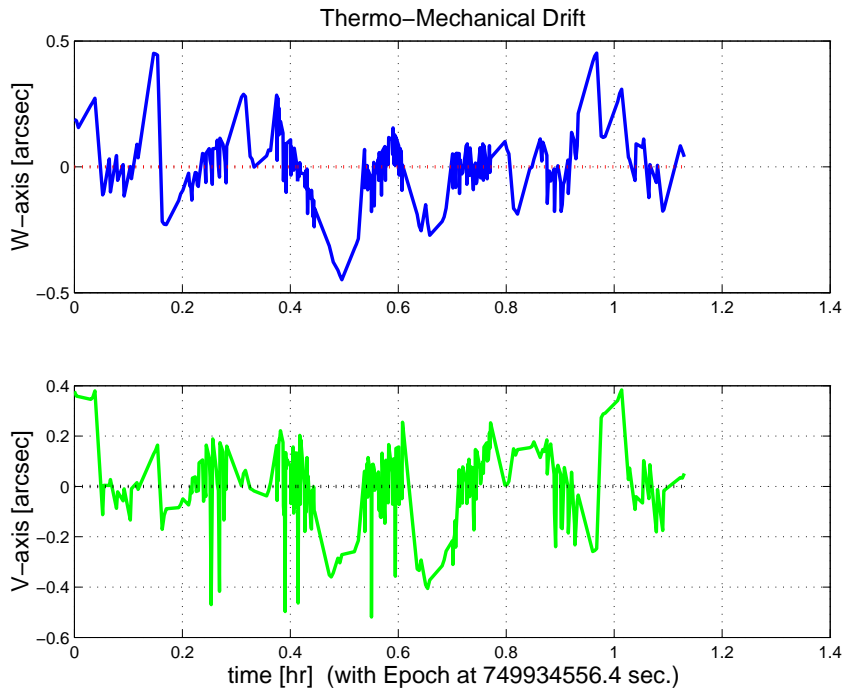


Figure 3.35: Thermo-mechanical boresight drift (equiv. angle in (W,V) coords)

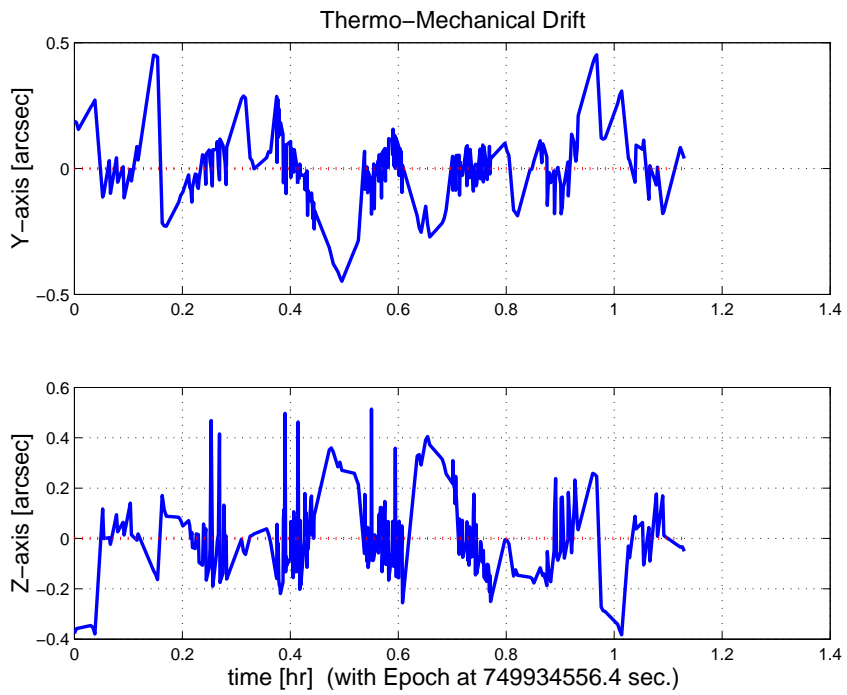


Figure 3.36: Thermo-mechanical boresight drift (equiv. angle in Body frame)

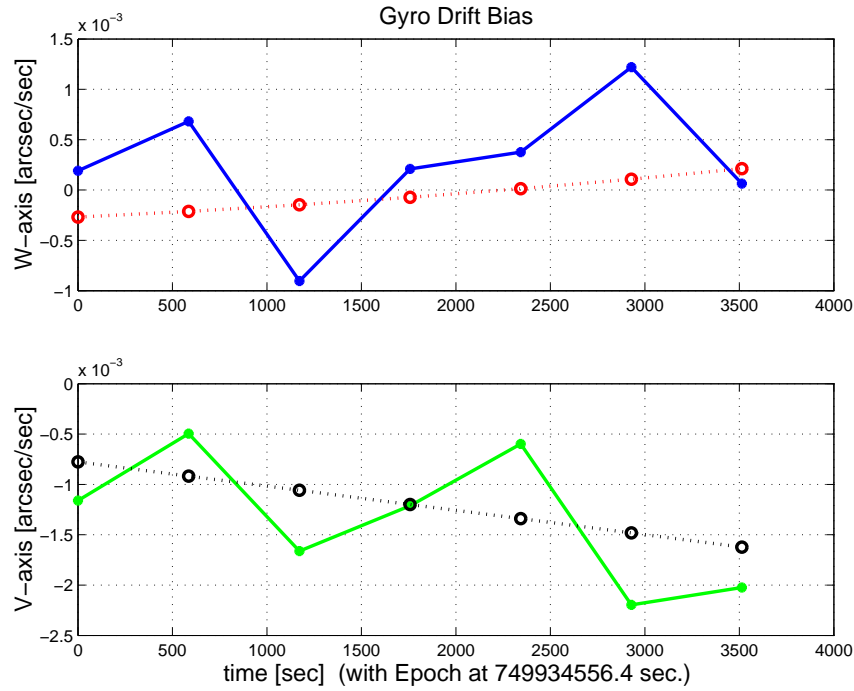


Figure 3.37: Gyro drift bias contribution (equiv. rate in (W,V) coords)

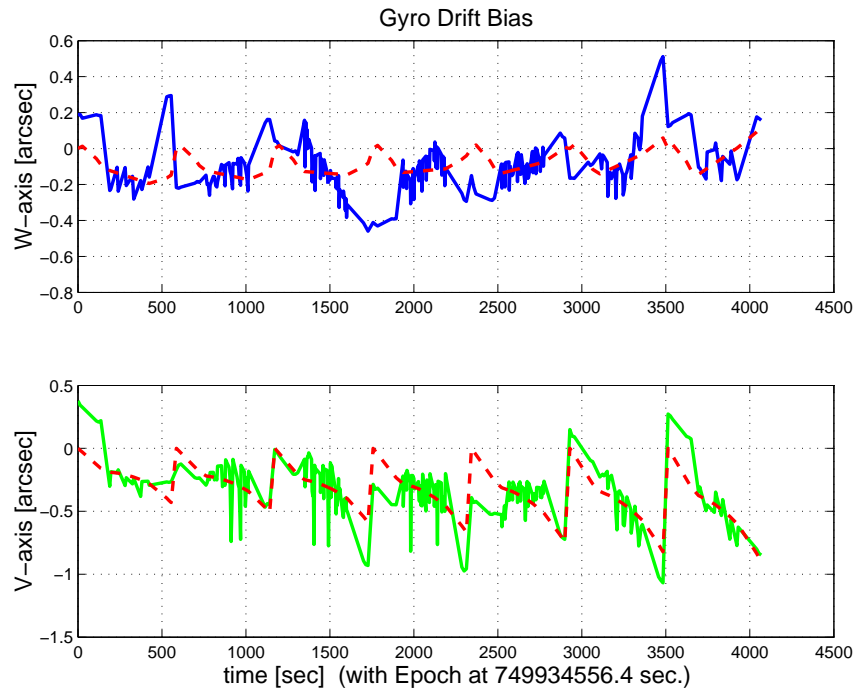


Figure 3.38: Gyro drift bias contribution (equiv. angle in (W,V) coords)

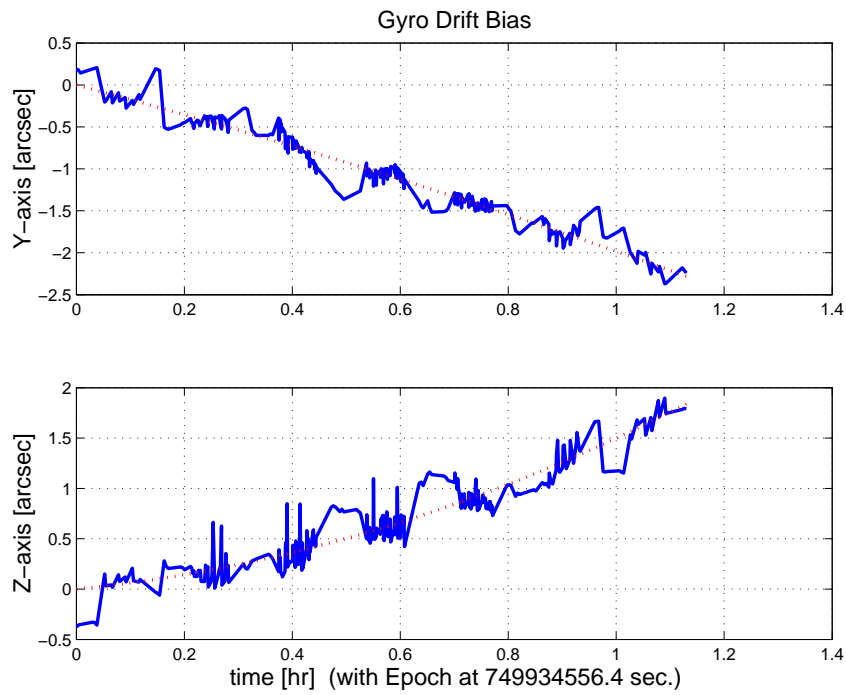


Figure 3.39: Gyro drift bias contribution (equiv. angle in Body frame)

3.2 IPF OUTPUT DATA (IF MINI FILE)

OUTPUT FILE NAME: IFmini001095.dat DATE: 17-Oct-2003 TIME: 16:53
 INSTRUMENT NAME: MIPS_24um_center NF: 95
 IPF FILTER VERSION: IPF.V2.0.0D SW RELEASE DATE: August 1, 2003
 FRAME TABLE USED: BodyFrames_SPC_08a

----- IPF BROWN ANGLE SUMMARY -----

Frame Number	WAS			IS		
	theta_Y (arcmin)	theta_Z (arcmin)	angle (deg)	theta_Y (arcmin)	theta_Z (arcmin)	angle (deg)
095	+6.724001	+4.258239	+0.577299	+6.718185	+4.247276	+0.638444
096	+6.721218	+6.970374	+0.577299	+6.695268	+7.063358	+0.638444
099	+7.758095	+4.277861	+0.577299	+7.758870	+4.260684	+0.638444
100	+5.669225	+4.238226	+0.577299	+5.661628	+4.235185	+0.638444
103	+6.827410	+4.260201	+0.577299	+6.822038	+4.248547	+0.638444
104	+6.641274	+4.256670	+0.577299	+6.635138	+4.246270	+0.638444

OFFSET	NF	Delta_CW	Delta_CV
0	95	+0.000	+0.000 pixels

OFFSET FRAME NAME: MIPS_24um_center

Brown Angle	theta_Y(arcmin)	theta_Z(arcmin)	angle(deg)
WAS(FTB)	+6.724001	+4.258239	+0.577299
IS (EST)	+6.718185	+4.247276	+0.638444
dT_EST	-0.005816	-0.010963	+0.061144
T_sSIGMA	+0.001223	+0.001103	+0.012693
dT_EST/T_sSIGMA	-4.754046	-9.943254	+4.817071

OFFSET	NF	Delta_CW	Delta_CV
1	96	+0.000	-64.000 pixels

OFFSET FRAME NAME: MIPS_24um_plusY_edge

Brown Angle	theta_Y(arcmin)	theta_Z(arcmin)	angle(deg)
WAS(FTB)	+6.721218	+6.970374	+0.577299
IS (EST)	+6.695268	+7.063358	+0.638444
dT_EST	-0.025950	+0.092984	+0.061144
T_sSIGMA	+0.001585	+0.001373	+0.012693
dT_EST/T_sSIGMA	-16.376267	+67.703517	+4.817075

OFFSET	NF	Delta_CW	Delta_CV
2	99	+25.000	+0.000 pixels

OFFSET FRAME NAME: MIPS_24um_small_FOV1

Brown Angle	theta_Y(arcmin)	theta_Z(arcmin)	angle(deg)
WAS(FTB)	+7.758095	+4.277861	+0.577299
IS (EST)	+7.758870	+4.260684	+0.638444
dT_EST	+0.000775	-0.017177	+0.061144
T_sSIGMA	+0.001238	+0.001135	+0.012693
dT_EST/T_sSIGMA	+0.626247	-15.133114	+4.817071

OFFSET	NF	Delta_CW	Delta_CV
3	100	-25.500	+0.000 pixels

OFFSET FRAME NAME: MIPS_24um_small_FOV2

Brown Angle	theta_Y(arcmin)	theta_Z(arcmin)	angle(deg)
WAS(FTB)	+5.669225	+4.238226	+0.577299
IS (EST)	+5.661628	+4.235185	+0.638444
dT_EST	-0.007597	-0.003040	+0.061144
T_sSIGMA	+0.001217	+0.001104	+0.012693
dT_EST/T_sSIGMA	-6.244673	-2.753512	+4.817071

OFFSET	NF	Delta_CW	Delta_CV
4	103	+2.500	+0.000 pixels

OFFSET FRAME NAME: MIPS_24um_large_FOV1

Brown Angle	theta_Y(arcmin)	theta_Z(arcmin)	angle(deg)
WAS(FTB)	+6.827410	+4.260201	+0.577299
IS (EST)	+6.822038	+4.248547	+0.638444

dT_EST	-0.005373	-0.011654	+0.061144	
T_sSIGMA	+0.001224	+0.001104	+0.012693	
dT_EST/T_sSIGMA	-4.387862	-10.556857	+4.817071	
OFFSET	NF	Delta_CW	Delta_CV	
5	104	-2.000	+0.000 pixels	
OFFSET FRAME NAME: MIPS_24um_large_FOV2				
Brown Angle	theta_Y(arcmin)	theta_Z(arcmin)	angle(deg)	
WAS(FTB)	+6.641274	+4.256670	+0.577299	
IS (EST)	+6.635138	+4.246270	+0.638444	
dT_EST	-0.006136	-0.010400	+0.061144	
T_sSIGMA	+0.001223	+0.001102	+0.012693	
dT_EST/T_sSIGMA	-5.019031	-9.439313	+4.817071	
VARNAME	MEAN	SIGMA	SCALED_SIGMA	
a00	-4.5631483650351325E-004	+1.3338404918099183E-004	+1.4078415769300782E-004	
b00	-5.7517044043127019E-004	+3.0084975840610734E-004	+3.1754081608271188E-004	
c00	-1.0281917404930513E-003	+1.9106510228217576E-004	+2.0166533895537030E-004	
a10	+5.3278896843793770E+000	+2.8171679370697927E-001	+2.9734636002986131E-001	
b10	+6.8771535607644374E-001	+7.1811635432891874E-001	+7.5795724219307747E-001	
c10	+7.5908531908626875E+000	+7.1103168422773022E-001	+7.5047951664153678E-001	
d10	-9.9601988628778848E-001	+3.0466329858338831E-001	+3.2156593036724246E-001	
a01	+7.6668355590843884E+000	+1.4757340851427464E-001	+1.5576073858259382E-001	
b01	+2.5138263439097468E+000	+3.9989981230095967E-001	+4.2208613835068381E-001	
c01	-1.5971199475298295E+001	+2.1272601657640774E-001	+2.2452799451650063E-001	
d01	-2.3652649475898331E+000	+1.7227565057094599E-001	+1.8183345389174085E-001	
e01	-2.0793237577454605E+001	+4.0498372033557489E-001	+4.2745210013424628E-001	
f01	+2.4792241563079731E+000	+2.3647193067594055E-001	+2.4959132506974382E-001	
del_alpha	+6.9800935864616775E-016	+2.3342363942100683E-004	+2.4637391549668099E-004	
beta	+9.6235334473005052E-001	+3.7273627844810553E-004	+3.9341557948760394E-004	
del_theta1	-4.7520581220039659E-015	+2.0989446877712882E-004	+2.2153935326339207E-004	
del_theta2	-8.0524973840853176E-018	+3.3714631802295598E-007	+3.5585109834051192E-007	
del_theta3	+1.6704522041259269E-017	+3.0387325754805143E-007	+3.2073205808351918E-007	
del_arx	+8.8933038450839108E-016	+7.0786719448003610E-005	+7.4713946191690660E-005	
del_ary	-8.9858284302860502E-018	+1.8260233374805136E-006	+1.9273305846798665E-006	
del_arz	+2.4651438091958318E-018	+1.8321738750055146E-006	+1.9338223522497771E-006	
bgx	+1.4588501599232332E-006	+1.5708528610656972E-006	+1.6580033239559293E-006	
bgy	-2.3082906003562955E-009	+2.0553796933962117E-009	+2.1694115649574603E-009	
bgz	+7.1164400698708779E-010	+2.7273953608253860E-009	+2.8787104674607384E-009	
cgx	+2.3043024642430984E-010	+5.4358711554179767E-010	+5.7374517166202174E-010	
cgy	-1.9507735802366981E-013	+1.0925726135269447E-012	+1.1531882264656805E-012	
cgz	+7.3841218185067421E-013	+1.0558413019852272E-012	+1.1144190723718259E-012	
LSQF RESIDUAL SIGMA SCALE =	+1.0554797110858032E+000			
a_mirror_ipf	+0.0000000000000000E+000	+1.2369426221784273E-002	+9.9992349572101968E-001	
a_mirror_tpf	-1.9527210038709274E-003	+1.2292116851814160E-003	+9.9999733795611412E-001	
beta	beta_0	beta	beta_total	
	+2.8047410000000001E-006	+9.6235334473005052E-001	+2.6991518824515068E-006	
qT	qT(1)	qT(2)	qT(3)	qT(4)
FrmTbl:	+5.0372558129468097E-003	-9.8107368935810191E-004	-6.1440075534372396E-004	+9.9998664294079498E-001
Estim:	+5.5708354382570388E-003	-9.8054664932168962E-004	-6.1228736020785908E-004	+9.9998381458150465E-001
DelTheta	deltheta(1)	deltheta(2)	deltheta(3)	
	+1.0671770433909459E-003	+1.7237789614618324E-006	+3.1719070281342866E-006	[rad]
EulAngT	theta(1)	theta(2)	theta(3)	[rad]
Mean	+1.1142943166700541E-002	-1.9542408971711632E-003	-1.2354825017054239E-003	
SigmaT	+2.0989446877712882E-004	+3.3714631802295598E-007	+3.0387325754805143E-007	
qR	qR(1)	qR(2)	qR(3)	qR(4)
ASFILE:	+7.0782797411084175E-004	+1.2707553105428815E-003	-1.6110119759105146E-004	+9.9999892711639404E-001
Estim:	+6.1824267536339441E-004	+1.2695077761671312E-003	-1.6037140276689942E-004	+9.9999899020299721E-001
DelThetaR	delthetaR(1)	delthetaR(2)	delthetaR(3)	

EulAngR	-1.7917194954967182E-004	-2.5229473426429052E-006	+1.2339185282886913E-006	[rad]
	angR(1)	angR(2)	angR(3)	[rad]
Mean	+1.2360812162895006E-003	+2.5392140139759685E-003	-3.1917378825308543E-004	
SigmaR	+7.0786719448003610E-005	+1.8260233374805136E-006	+1.8321738750055146E-006	
<hr/>				
Initial Gyro Bias	Bg0(1)	Bg0(2)	Bg0(3)	
	+3.8798614809820720E-007	+1.7442596345063063E-007	-3.4433065820849146E-007	
Gyro Bias Correction	Bg(1)	Bg(2)	Bg(3)	
	+1.4588501599232332E-006	-2.3082906003562955E-009	+7.1164400698708779E-010	
Total Gyro Bias	BgT(1)	BgT(2)	BgT(3)	
	+1.8468363080214403E-006	+1.7211767285027434E-007	-3.4361901420150440E-007	
<hr/>				
Initial Gyro Bias Rate	Cg0(1)	Cg0(2)	Cg0(3)	
	+0.0000000000000000E+000	+0.0000000000000000E+000	+0.0000000000000000E+000	
Gyro Bias Rate Correction	Cg(1)	Cg(2)	Cg(3)	
	+2.3043024642430984E-010	-1.9507735802366981E-013	+7.3841218185067421E-013	
Total Gyro Bias Rate	CgT(1)	CgT(2)	CgT(3)	
	+2.3043024642430984E-010	-1.9507735802366981E-013	+7.3841218185067421E-013	
<hr/>				
OFFSET	NF	Delta_CW	Delta_CV	
1	96	+0.000	-64.000	pixels
OFFSET FRAME NAME:	MIPS_24um_plusY_edge			
qT	qT(1)	qT(2)	qT(3)	qT(4)
WAS(FTB)	+5.0368688350518696E-003	-9.8265590121642096E-004	-1.0088615259627000E-003	+9.9998632317554204E-001
IS (EST)	+5.5704367984730288E-003	-9.7949520074086635E-004	-1.0218817857010993E-003	+9.9998348315391783E-001
<hr/>				
DelTheta	deltheta(1)	deltheta(2)	deltheta(3)	
Units	rad	rad	rad	
	+1.0671179272267091E-003	+7.2756351445502054E-006	-2.7122483067172369E-005	
EulAngT	theta(1)	theta(2)	theta(3)	[rad]
Mean	+1.1142943166700541E-002	-1.9475746205400240E-003	-2.0546475894192605E-003	
sSigmaT	+2.2153918499755209E-004	+4.6094399774150730E-007	+3.9950437695847479E-007	
SigmaT	+2.0989430935593084E-004	+4.3671516647849214E-007	+3.7850502739412473E-007	
<hr/>				
OFFSET	NF	Delta_CW	Delta_CV	
2	99	+25.000	+0.000	pixels
OFFSET FRAME NAME:	MIPS_24um_small_FOV1			
qT	qT(1)	qT(2)	qT(3)	qT(4)
WAS(FTB)	+5.0371586372862228E-003	-1.1314889056829706E-003	-6.1649671362086034E-004	+9.9998648325740958E-001
IS (EST)	+5.5707388424245064E-003	-1.1319165308581653E-003	-6.1339397774659132E-004	+9.9998365455718563E-001
<hr/>				
DelTheta	deltheta(1)	deltheta(2)	deltheta(3)	
Units	rad	rad	rad	
	+1.0671820818558223E-003	-1.7514849635406710E-007	+4.9986352228126053E-006	
EulAngT	theta(1)	theta(2)	theta(3)	[rad]
Mean	+1.1142943166700539E-002	-2.2569638591662892E-003	-1.2393825998013033E-003	
sSigmaT	+2.2153933287104183E-004	+3.6008791197714243E-007	+3.3017853420496915E-007	
SigmaT	+2.0989444945667196E-004	+3.4116042989278245E-007	+3.1282319379242707E-007	
<hr/>				
OFFSET	NF	Delta_CW	Delta_CV	
3	100	-25.500	+0.000	pixels
OFFSET FRAME NAME:	MIPS_24um_small_FOV2			
qT	qT(1)	qT(2)	qT(3)	qT(4)
WAS(FTB)	+5.0373539303327245E-003	-8.2765014547835373E-004	-6.1226286617559059E-004	+9.9998678251004891E-001
IS (EST)	+5.5709325898909414E-003	-8.2686934353415602E-004	-6.1138512180013941E-004	+9.9998395347395475E-001
<hr/>				
DelTheta	deltheta(1)	deltheta(2)	deltheta(3)	
Units	rad	rad	rad	
	+1.0671722641028528E-003	+2.2186644793782625E-006	+8.6208602961888918E-007	
EulAngT	theta(1)	theta(2)	theta(3)	[rad]
Mean	+1.1142943166700541E-002	-1.6469009241840771E-003	-1.2319654714847928E-003	
sSigmaT	+2.2153935314390716E-004	+3.5388015113679975E-007	+3.2118906635972370E-007	
SigmaT	+2.0989446866392448E-004	+3.3527897070873374E-007	+3.0430624386830420E-007	
<hr/>				

OFFSET NF Delta_CW Delta_CV
 4 103 +2.500 +0.000 pixels
 OFFSET FRAME NAME: MIPS_24um_large_FOV1
 qT qT(1) qT(2) qT(3) qT(4)
 WAS(FTB) +5.0372461391393897E-003 -9.9611521251996506E-004 -6.1461035168427895E-004 +9.9998662799056104E-001
 IS (EST) +5.5708258405811261E-003 -9.9565218896179985E-004 -6.1238812774753505E-004 +9.9998379964725104E-001

DelTheta deltheta(1) deltheta(2) deltheta(3)
 Units rad rad rad
 +1.0671775383011436E-003 +1.5968748685018884E-006 +3.3740858962661747E-006
 EulAngT theta(1) theta(2) theta(3) [rad]
 Mean +1.1142943166700541E-002 -1.9844504053522557E-003 -1.2358523715840183E-003
 sSigmaT +2.2153935214267053E-004 +3.5616383333283118E-007 +3.2111933749249559E-007
 SigmaT +2.0989446771531634E-004 +3.3744261456853104E-007 +3.0424018019460613E-007

OFFSET NF Delta_CW Delta_CV
 5 104 -2.000 +0.000 pixels
 OFFSET FRAME NAME: MIPS_24um_large_FOV2
 qT qT(1) qT(2) qT(3) qT(4)
 WAS(FTB) +5.0372635449913205E-003 -9.6904047066332906E-004 -6.1423307818932811E-004 +9.9998665473808712E-001
 IS (EST) +5.5708431067704916E-003 -9.6846724945368219E-004 -6.1220832924998865E-004 +9.9998382635882077E-001

DelTheta deltheta(1) deltheta(2) deltheta(3)
 Units rad rad rad
 +1.0671766499396897E-003 +1.8152240486598044E-006 +3.0070429672854445E-006
 EulAngT theta(1) theta(2) theta(3) [rad]
 Mean +1.1142943166700539E-002 -1.9300833368531326E-003 -1.2351898281893709E-003
 sSigmaT +2.2153935401373698E-004 +3.5561326394840407E-007 +3.2048788761153380E-007
 SigmaT +2.0989446948803297E-004 +3.3692098503965957E-007 +3.0364192153143182E-007

q(1) q(2) q(3) q(4)
 PCRS1A: +5.3377191730804340E-007 +3.7444181445836429E-004 -1.4255121007937610E-003 +9.9999891385355677E-001
 PCRS2A: -5.2784857378083422E-007 +3.8463011681657313E-004 +1.3723523317471205E-003 +9.9999898435372037E-001

***** CS-FILE PARAMETERS: ***** AS-FILE PARAMETERS: *****

Row (01) PIX2RADX: +1.2087416876100000E-005 Row (1) TASTART: +7.4993345329074097E+008
 Row (02) PIX2RADY: +1.2595908372599999E-005 Row (2) TASTOP: +7.4993958719077146E+008
 Row (03) CX0: +6.450000000000000000E+001 Row (3) S/C TIME: +7.4938219429075623E+008
 Row (04) CY0: +6.450000000000000000E+001 Row (4) QR1: +7.0782797411084175E-004
 Row (05) BETA0: +2.8047410000000001E-006 Row (5) QR2: +1.2707553105428815E-003
 Row (06) GAMMA_E0: +2.0070000000000000E+003 Row (6) QR3: -1.6110119759105146E-004
 Row (07) D11: -1.0000000000000000E+000 Row (7) QR4: +9.9999892711639404E-001
 Row (08) D12: +0.0000000000000000E+000
 Row (09) D21: +0.0000000000000000E+000
 Row (10) D22: -1.0000000000000000E+000
 Row (11) DG: -1.0000000000000000E+000

INITIAL STA-TO-PCRS ALIGNMENT (R) KNOWLEDGE (1-SIGMA)

SIGMA(X)	SIGMA(Y)	SIGMA(Z)
4.71429223E+000	2.15487256E-001	2.15829050E-001 [arcsec]

PIX2RADX = 1.208741687610E-005 [rad/pixel]
 XPIXSIZE = 2.4932 [arcsec]
 PIX2RADY = 1.259590837260E-005 [rad/pixel]
 YPIXSIZE = 2.5981 [arcsec]
 CX0 = 64.5 [pixel] = 160.81 [arcsec]
 CY0 = 64.5 [pixel] = 167.58 [arcsec]

NOMINAL BETA0 = 2.804741000000E-006 [rad/encoder unit]
 ENCODER UNIT SIZE = 0.58 [arcsec]
 GAMMA_E0 = 2007.00 [encoder unit] = 1161.09 [arcsec]

| -1 | +0 |
 FLIP MATRIX D = |----|----| and DG = -1
 | +0 | -1 |

3.3 IPF EXECUTION LOG

```
*****
IPF EXECUTION-LOG FILE NAME: LG001095.dat
INSTRUMENT TYPE: MIPS_24um_center
IPF FILTER EXECUTION DATE: 17-Oct-2003 TIME: 16:48
IPF FILTER VERSION USED: IPF.V2.0.0D
*****
```

```
----- Loading & Preparing Input Files -----
AAFILE: AA001095 Loaded! AAFILE dimension = 61340 X 21
ASFILE: AS001095 Loaded!
CAFILe: CA003095 Loaded! CAFILe dimension = 227 X 15
CBFILE: CB002095 Loaded! CBFILE dimension = 63 X 15
CCFILE: CC001095 Created! CCFILE dimension = 290 X 19
CSFILE: CS003095 Loaded!
Loading Input Files Completed!
```

```
----- Selected Mask Vectors -----
index = 1 2 3 4 5 6 7 8 9 10 11 12 13 14 15 16 17 18 19 20
-----
mask1 = [ 1 1 1 1 1 1 1 0 0 0 0 1 1 1 1 1 1 1 ]
mask2 = [ 1 1 1 1 1 1 1 0 0 0 0 0 0 1 1 1 1 1 ]
```

```
----- Selected Initial Gyro Bias Parameters -----
User Entered 1 : Use AFILE database - from S/C filter
IPF Linearized Using Following Nominal Gyro Bias Estimates
bg0 = [+3.8798614809820720E-007 +1.7442596345063063E-007 -3.4433065820849146E-007 ]
cg0 = [+0.0000000000000000E+000 +0.0000000000000000E+000 +0.0000000000000000E+000 ]
```

```
----- Gyro Pre-Processor Run Completed -----
AGFILE CREATED: AG001095.m ACFILE CREATED: AC001095.m
```

```
Total Gyro Preprocessor Execution Time: 29 seconds
```

```
FRAME TABLE ENTRIES FOR PCRS LOADED TO TPCRS
q_PCRS4 = [ +5.3377191730804340E-007 q_PCRS5 = [ +7.3379987833742897E-007
+3.7444181445836429E-004 +5.2236196154513707E-004
-1.4255121007937610E-003 -1.4047712280184723E-003
+9.999891385355677E-001 ]; +9.999887687698918E-001 ];
q_PCRS8 = [ -5.2784857378083422E-007 q_PCRS9 = [ -7.1963421681856818E-007
+3.8463011681657313E-004 +5.3239763239987400E-004
+1.3723523317471205E-003 +1.3516841804518383E-003
+9.9999898435372037E-001 ]; +9.9999894475050310E-001 ];

----- Initial Conditions for State ----- ----- Initial Square-Root Cov (diag) -----
p1(01) = a00 = +0.0000000000000000E+000 Sigma_initial(01,01) = 1.0000000000000000E+000
p1(02) = b00 = +0.0000000000000000E+000 Sigma_initial(02,02) = 1.0000000000000000E+000
p1(03) = c00 = +0.0000000000000000E+000 Sigma_initial(03,03) = 1.0000000000000000E+000
p1(04) = a10 = +0.0000000000000000E+000 Sigma_initial(04,04) = 1.0000000000000000E+002
p1(05) = b10 = +0.0000000000000000E+000 Sigma_initial(05,05) = 1.0000000000000000E+002
p1(06) = c10 = +0.0000000000000000E+000 Sigma_initial(06,06) = 1.0000000000000000E+002
p1(07) = d10 = +0.0000000000000000E+000 Sigma_initial(07,07) = 1.0000000000000000E+002
p1(08) = a20 = +0.0000000000000000E+000 Sigma_initial(08,08) = 9.9999000000000000E+004
p1(09) = b20 = +0.0000000000000000E+000 Sigma_initial(09,09) = 9.9999000000000000E+004
```

```

p1(10) = c20 = +0.0000000000000000E+000 Sigma_initial(10,10) = 9.999900000000000E+004
p1(11) = d20 = +0.0000000000000000E+000 Sigma_initial(11,11) = 9.999900000000000E+004
p1(12) = a01 = +0.0000000000000000E+000 Sigma_initial(12,12) = 1.000000000000000E+004
p1(13) = b01 = +0.0000000000000000E+000 Sigma_initial(13,13) = 1.000000000000000E+004
p1(14) = c01 = +0.0000000000000000E+000 Sigma_initial(14,14) = 1.000000000000000E+004
p1(15) = d01 = +0.0000000000000000E+000 Sigma_initial(15,15) = 1.000000000000000E+004
p1(16) = e01 = +0.0000000000000000E+000 Sigma_initial(16,16) = 1.000000000000000E+004
p1(17) = f01 = +0.0000000000000000E+000 Sigma_initial(17,17) = 1.000000000000000E+004
-----
p2f(01) = am1 = +0.0000000000000000E+000 Sigma_initial(18,18) = 1.0000000000000001E-001
p2f(02) = am2 = +0.0000000000000000E+000 Sigma_initial(19,19) = 1.0000000000000001E-001
p2f(03) = am3 = +1.0000000000000000E+000 Sigma_initial(20,20) = 1.0000000000000001E-001
p2f(04) = beta = +1.0000000000000000E+000 Sigma_initial(21,21) = 1.0000000000000000E-002
p2f(05) = qT1 = +5.0372558129468141E-003 Sigma_initial(22,22) = 1.0000000000000000E-002
p2f(06) = qT2 = -9.8107368935810278E-004 Sigma_initial(23,23) = 2.2855533686591019E-004
p2f(07) = aT3 = -6.1440075534372450E-004 Sigma_initial(24,24) = 1.0447116979821692E-005
p2f(08) = qT4 = +9.9998664294079587E-001 Sigma_initial(25,25) = 1.0463687644985126E-005
p2f(09) = qR1 = +7.0782797411084175E-004 Sigma_initial(26,26) = 9.999900000000000E+004
p2f(10) = qR2 = +1.2707553105428815E-003 Sigma_initial(27,27) = 9.999900000000000E+004
p2f(11) = qR3 = -1.6110119759105146E-004 Sigma_initial(28,28) = 9.999900000000000E+004
p2f(12) = qR4 = +9.9999892711639404E-001 Sigma_initial(29,29) = 9.999900000000000E+004
p2f(13) = brx = +0.0000000000000000E+000 Sigma_initial(30,30) = 9.999900000000000E+004
p2f(14) = bry = +0.0000000000000000E+000 Sigma_initial(31,31) = 9.999900000000000E+004
p2f(15) = brz = +0.0000000000000000E+000 Sigma_initial(32,32) = 2.4585125629856917E-004
p2f(16) = crx = +0.0000000000000000E+000 Sigma_initial(33,33) = 2.4585125629856917E-004
p2f(17) = cry = +0.0000000000000000E+000 Sigma_initial(34,34) = 2.4585125629856917E-004
p2f(18) = crz = +0.0000000000000000E+000 Sigma_initial(35,35) = 6.0442840223584758E-008
p2f(19) = bgx = +0.0000000000000000E+000 Sigma_initial(36,36) = 6.0442840223584758E-008
p2f(20) = bgy = +0.0000000000000000E+000 Sigma_initial(37,37) = 6.0442840223584758E-008
p2f(21) = bgz = +0.0000000000000000E+000 Sigma_initial(38,38) = 6.0442840223584758E-008
p2f(22) = cgx = +0.0000000000000000E+000 Sigma_initial(39,39) = 6.0442840223584758E-008
p2f(23) = cgy = +0.0000000000000000E+000 Sigma_initial(40,40) = 6.0442840223584758E-008
p2f(24) = cgz = +0.0000000000000000E+000 Sigma_initial(41,41) = 6.0442840223584758E-008
-----

```

```

----- IPF KALMAN FILTER STARTED -----
Iteration#001: |dp|= +2.923388906087E+001 RMS(|Res|)=+1.263420341113E-005
Iteration#002: |dp|= +3.858069924280E-002 RMS(|Res|)=+3.458261468810E-006
Iteration#003: |dp|= +8.135580395357E-003 RMS(|Res|)=+1.857705116763E-006
Iteration#004: |dp|= +3.720174933893E-003 RMS(|Res|)=+1.837909443886E-006
Iteration#005: |dp|= +4.026198439453E-005 RMS(|Res|)=+1.835089495760E-006
Iteration#006: |dp|= +3.572071580738E-004 RMS(|Res|)=+1.835513614107E-006
Iteration#007: |dp|= +7.484717612068E-005 RMS(|Res|)=+1.835609380301E-006
Iteration#008: |dp|= +1.932631415950E-005 RMS(|Res|)=+1.835601464970E-006
Iteration#009: |dp|= +1.108714693758E-005 RMS(|Res|)=+1.835599066272E-006
Iteration#010: |dp|= +4.007790316182E-007 RMS(|Res|)=+1.835599491009E-006
Iteration#011: |dp|= +9.854353929778E-007 RMS(|Res|)=+1.835599559417E-006
Iteration#012: |dp|= +2.369416479233E-007 RMS(|Res|)=+1.835599511436E-006
Iteration#013: |dp|= +4.669538442751E-008 RMS(|Res|)=+1.835599501356E-006
Iteration#014: |dp|= +3.216327688216E-008 RMS(|Res|)=+1.835599504983E-006
Iteration#015: |dp|= +2.058164015948E-009 RMS(|Res|)=+1.835599506577E-006
Iteration#016: |dp|= +2.678714638851E-009 RMS(|Res|)=+1.835599506494E-006
Iteration#017: |dp|= +7.088286598531E-010 RMS(|Res|)=+1.835599506334E-006
Iteration#018: |dp|= +1.146764322744E-010 RMS(|Res|)=+1.835599506306E-006
Iteration#019: |dp|= +1.173380003192E-010 RMS(|Res|)=+1.835599506319E-006
Iteration#020: |dp|= +8.867601264758E-011 RMS(|Res|)=+1.835599506320E-006
Iteration#021: |dp|= +1.034337608083E-010 RMS(|Res|)=+1.835599506330E-006
Iteration#022: |dp|= +4.294929288901E-011 RMS(|Res|)=+1.835599506319E-006
Iteration#023: |dp|= +5.533254747774E-011 RMS(|Res|)=+1.835599506317E-006
Iteration#024: |dp|= +7.371086871788E-011 RMS(|Res|)=+1.835599506320E-006
Iteration#025: |dp|= +5.640050254276E-011 RMS(|Res|)=+1.835599506324E-006
Iteration#026: |dp|= +9.805338326027E-011 RMS(|Res|)=+1.835599506323E-006
Iteration#027: |dp|= +5.364746679925E-011 RMS(|Res|)=+1.835599506320E-006
Iteration#028: |dp|= +1.250474616073E-010 RMS(|Res|)=+1.835599506326E-006
Iteration#029: |dp|= +6.057809671472E-011 RMS(|Res|)=+1.835599506315E-006
Iteration#030: |dp|= +7.013390751722E-011 RMS(|Res|)=+1.835599506314E-006
IPF Kalman Filter Completed with Error |dp1| + |dp2| = +7.0133907517224141E-011
-----
```

```

----- IPF LEAST SQUARES FILTER STARTED -----
Iteration#001 COND#=+2.241783314396E+009, |dp|=+2.923244960994E+001
Iteration#002 COND#=+2.241837830694E+009, |dp|=+2.742962119457E-002
Iteration#003 COND#=+2.241837921822E+009, |dp|=+1.131932286882E-003
Iteration#004 COND#=+2.241837934419E+009, |dp|=+2.786972451794E-005
Iteration#005 COND#=+2.241837933467E+009, |dp|=+3.639443929191E-007
Iteration#006 COND#=+2.241837930999E+009, |dp|=+4.547957415594E-009
Iteration#007 COND#=+2.241837931670E+009, |dp|=+1.863471791048E-010
Iteration#008 COND#=+2.241837931036E+009, |dp|=+1.659433592044E-010
Iteration#009 COND#=+2.241837938096E+009, |dp|=+7.392008244009E-011
Iteration#010 COND#=+2.241837920784E+009, |dp|=+5.737788159571E-011
Iteration#011 COND#=+2.241837931601E+009, |dp|=+7.943787703054E-011
Iteration#012 COND#=+2.241837930092E+009, |dp|=+7.785593879279E-011
Iteration#013 COND#=+2.241837928544E+009, |dp|=+8.032647097817E-011
Iteration#014 COND#=+2.241837913887E+009, |dp|=+1.045905604328E-010
Iteration#015 COND#=+2.241837934703E+009, |dp|=+9.728263571348E-011
Iteration#016 COND#=+2.241837934492E+009, |dp|=+3.904117803119E-011
Iteration#017 COND#=+2.241837916185E+009, |dp|=+7.049777087051E-011
Iteration#018 COND#=+2.241837931420E+009, |dp|=+8.562747042633E-011
Iteration#019 COND#=+2.241837919051E+009, |dp|=+1.026086601150E-010
Iteration#020 COND#=+2.241837935361E+009, |dp|=+7.829338403282E-011
Iteration#021 COND#=+2.241837950348E+009, |dp|=+9.657880804700E-011
Iteration#022 COND#=+2.241837924051E+009, |dp|=+6.240762424867E-011
Iteration#023 COND#=+2.241837932627E+009, |dp|=+8.858056834637E-011
Iteration#024 COND#=+2.241837917653E+009, |dp|=+9.290808205005E-011
Iteration#025 COND#=+2.241837921687E+009, |dp|=+9.106463191514E-011
Iteration#026 COND#=+2.241837941935E+009, |dp|=+6.850803194340E-011
Iteration#027 COND#=+2.241837932393E+009, |dp|=+7.287268794382E-011
Iteration#028 COND#=+2.241837939396E+009, |dp|=+6.498314953930E-011
Iteration#029 COND#=+2.241837942302E+009, |dp|=+1.178951062537E-010
Iteration#030 COND#=+2.241837925631E+009, |dp|=+1.045577717947E-010
IPF Least Squares Filter Completed with Error |dp1| + |dp2| = +1.0455777179468052E-010
-----
```

Total Execution Time: 280 seconds

4 COMMENTS

The data set looked clean and filter converged nicely. Comments:

1. The run was performed in normal IPF operating mode. This decision was made based on seeing systematic errors at about 0.4 arcseconds in the observer at centroid times, implying that Lite Mode 3 (observer-based) would not be adequate.
2. This run estimated 27 total parameters consisting of: 3 constant and 6 linear plate scales, 4 Gamma Dependent parameters, 2 mirror parameters, 3 IPF alignment angles, 3 STA-to-PCRS alignment angles, and 3 gyro bias and 3 gyro bias-drift parameters.
3. Amy Mainzer has indicated that the PCRS measurements for this run were based on a simple center-of-mass algorithm which was accurate to about 0.5 arcseconds (looked like .4" average), which will limit the accuracy of this IPF run. The errors on the PCRS appeared mostly systematic and field dependent, being repeatable and larger the further they were located from the center. This will further limit the accuracy of the IPF run.
4. The linear plate scales were helpful in this run to estimate centroids accurately (see quiver plots in Figures 3-28 through 3-32). The constant plate scales were much smaller than the linear terms.
5. The scan mirror parameter estimates indicate that the mirror spin axis is tilted by 0.7 deg and the scan mirror scale factors are off by 4 percent.
6. There were 227 science centroids in the science data set, and 63 PCRS measurements. The data set was coordinated as 7 sandwich maneuvers. The number of science and PCRS centroids was sufficient to identify all 27 parameters.
7. This run was made using BodyFrames_SPC_08a which was a special frame table incorporating the 40 star Stage 2 PAC filter run results.

We recommend updating frames 95, 96, 99, 100, 103 and 104 with the new quaternions listed in the IF file IF001095.dat. This contains adjustments of 0.35 and 0.6 arcseconds in Y and Z, and .06 deg in twist (for the prime frame). In our best judgment, these frames will be accurate to better than 0.3 arcsecond (disregard the accuracies quoted in the tables).

IPF TEAM CONTACT INFORMATION

IPF Team email	ipf@sirtfweb.jpl.nasa.gov	
David S. Bayard	X4-8208	David.S.Bayard@jpl.nasa.gov (TEAM LEADER)
Dhemetrio Boussalis	X4-3977	boussali@grover.jpl.nasa.gov
Paul Brugarolas	X4-9243	Paul.Brugarolas@jpl.nasa.gov
Bryan H. Kang	X4-0541	Bryan.H.Kang@jpl.nasa.gov
Edward.C.Wong	X4-3053	Edward.C.Wong@jpl.nasa.gov (TASK MANAGER)

ACKNOWLEDGEMENTS

This work was performed at the Jet Propulsion Laboratory, California Institute of Technology, under contract with the National Aeronautics and Space Administration.

References

- [1] D.S. Bayard, B.H. Kang, *SIRTF Instrument Pointing Frame Kalman Filter Algorithm*, JPL D-Document D-24809, September 30, 2003.
- [2] B.H. Kang, D.S. Bayard, *SIRTF Instrument Pointing Frame (IPF) Software Description Document and User's Guide*, JPL D-Document D-24808, September 30, 2003.
- [3] D.S. Bayard, B.H. Kang, *SIRTF Instrument Pointing Frame (IPF) Kalman Filter Unit Test Report*, JPL D-Document D-24810, September 30, 2003.
- [4] *Space Infrared Telescope Facility In-Orbit Checkout and Science Verification Mission Plan*, JPL D-Document D-22622, 674-FE-301 Version 1.4, February 8, 2002.
- [5] *Space Infrared Telescope Facility Observatory Description Document*, Lockheed Martin LMMS/P458569, 674-SEIT-300 Version 1.2, November 1, 2002.
- [6] *SIRTF Software Interface Specification for Science Centroid INPUT Files (CAFILER, CSFILE)*, JPL SOS-SIS-2002, November 18, 2002.
- [7] *SIRTF Software Interface Specification for Inferred Frames Offset INPUT Files (OFILE)*, JPL SOS-SIS-2003, November 18, 2002.
- [8] *SIRTF Software Interface Specification for PCRS Centroid INPUT Files (CBFILE)*, JPL SIS-FES-015, November 18, 2002.
- [9] *SIRTF Software Interface Specification for Attitude INPUT Files (AFILE, ASFILE)*, JPL SIS-FES-014, January 7, 2002.
- [10] *SIRTF Software Interface Specification for IPF Filter Output Files (IFFILE, LGFILE, TARFILE)*, JPL SOS-SIS-2005, November 18, 2002.
- [11] R.J. Brown, *Focal Surface to Object Space Field of View Conversion*. Systems Engineering Report SER No. S20447-OPT-051, Ball Aerospace & Technologies Corp., November 23, 1999.